UNIVERSITAT POLITÈCNICA DE VALÈNCIA

TELECOM ESCUELA TÉCNICA VLC SUPERIOR DE INGENIERÍA DE TELECOMUNICACIÓN

Extension to Two Dimensions of Ultra-dense Network Analytical Model

Liu Yilin

Jose F. Monserrat and Daniel Clabuig

Bachelor's Thesis presented at Escuela Técnica Superior de Ingenieros de Telecomunicación of Universitat Politècnica de València,

Academic Year 2019-2020

Valencia, 5 de March de 2020

Escuela Técnica Superior de Ingeniería de Telecomunicación
Universitat Politècnica de València
Edificio 4D. Camino de Vera, s/n, 46022 Valencia
Tel. +34 96 387 71 90, ext. 77190
www.etsit.upv.es

VLC/ CAMPUS
VALENCIA, INTERNATIONAL CAMPUS OF EXCELLENCE

EMAS
Gestión ambiental verificada
REG.NO. ES-CV- 000030

Table of Contents

Abstract

With the development of society and technology, and the emergence of the Fifth-Generation Mobile Wireless networks, people's demand for communication speed and connectivity is increasing greatly. And there are several methods to improve the performance of the 5G networks, which are the increase of the spectral efficiency, the use of larger amounts of spectrum such as millimetre wave band [1], and the use of much more base stations per unit area which means to increase the densification.

This article considers the third method which is increasing the densification as the main driving force for the high transmission speed required in the future 5G networks. As for this purpose, this paper focuses on ultra-dense networks (UDN).

Firstly, this paper expresses a network model mathematically which is 2D. The network model contains infinite base stations and infinite user equipment and both of them are arranged periodically. And then, because of its periodicity, we can just analyse the performance and the mathematical expression of one of them. And based on the mathematical expression, how to optimize the resource and power allocation is figured out. Finally, the performance limits of 2D ultra-dense networks also can be analysed by using the outcomes of the previous work.

Chapter 1: Introduction

The arrival of the 4G era has brought an overwhelming network, let us be surrounded by the network, such as wireless WiFi, TV boxes and other wireless tools around people, madding people's lives full of convenience, in the 5G era, the network has become faster and faster, which just satisfies the increasing demand of people. And also, with the development of Fifth-Generation wireless networks, the ear of the Internet of Things has quietly entered our lives. The premise of the Internet of Everything is the foundation of the popularity of the network, and higher network configuration and faster network transmission are required, but luckily, 5G can provide these precisely. This paper mainly considers the ultra-dense networks (UDNs), generally defined as those networks who contain more base stations than active users.

As for the ultra-dense networks, if we decrease the distance between the base station the user, the average radio link quality would be increase since the path loss would be decreased. While, at the same time, the interference would be increased from the non-serving base stations. So, this paper establishes a system model to find out what is the best distance between base station and user equipment which means at which place, the performance of the network is the best.

So, we decided to analyse the performance of 5G network, and to find out under which circumstances the ultra-dense network would have a best performance. Because of the destination, we build an analytical model firstly, which is two dimensional. The two dimension means there is a layer which is full of infinite base stations and there is another layer full of user equipment. User equipment could be mobile phones or laptops. By the way, these two layers and are parallel and separated h meters. So, the minimum distance between one base station and a user is h meters. And then, we build a coordinate system to put both of base station layer and user equipment layer into it to express the model clearer and easier to understand. We set the model is periodic, the distance between two closest base stations is fixed, and similarly, the distance between two closest user equipment is fixed, so we can just express one of clusters, because they the same. After express the location of base stations and user equipment, we can find the mathematical expression of path loss value by using the distance expression between a specific base station which transmit to a specific user equipment. Then we come to the most important part which are three related elements: signal power, interference term, and the achievable rate. At this time, we use the Barnes' multiple zeta function [2] to express the interference term. Since the Barnes' multiple zeta function is convergence, which means the interference term is also convergence, indicating the interference is limited and would not be

infinite with the distance between base stations decreasing. So, if we have the expression of signal power, the interference term, and the achievable rate, we are able to draw the related figures, such as we could see what the performance would be if we decrease the distance between the base stations until the distance nearly equals to 0, or to see which type of cluster would be better, the overlapped or the non-overlapped.

Chapter 2: Background

With the development of technology, much ink has been spilled about Fifth-Generation wireless network. With the increasing demand of digital users for speed and connectivity, network densification is very important for 5G. And to satisfy this advantage, the distance between base stations is decreased and this increases the available network capacity by adding more cellular base stations (including wireless access network, macro base station, indoor wireless and small base station deployment).

More and more network connected devices and the wide variety of service requirements attached to them have brought great pressure to the current 4G network. Therefore, new enhancements must be added to the available features in 4G networks in the next generation of wireless systems. To this end, industry partners and academia are working together to define 5G system concept. As we conceive, the requirements of 5G network are various. Indeed, although the most important service requirements for road safety applications are reliability and low latency, large-scale connection of equipment is more important for smart cities. In order to integrate the requirements of all possible scenarios, because different application scenarios need different performance, 5G network needs to meet. Then the following points summarize the various requirements that 5G network needs to support [3]:

1. 1 to 10 Gbps data rates in real networks, what implies 10 times increase from the theoretical peak data rate in LTE networks.
2. 1ms end to end latency.
3. Higher bandwidth per area.
4. Enormous number of connected devices to support the emerging IoT.
5. Perceived availability of 99.999% of the time.
6. Almost 100% coverage for anywhere connectivity.
7. Reduction in energy usage by almost 90% to support the progressive introduction of green communications.
8. High battery life for the devices, by reducing their power consumption.

A one-dimensional ultra-dense network analytical model has been proposed because of the tendency of the 5G [4]. The model firstly has a very detailed description of the model which is

periodic and is composed of infinite base stations which transmit to infinite users. The base station and user equipment are deployed in two parallel lines. And the fixed number of base stations and user equipment are deployed into infinite clusters respectively. Cluster, is a new technology to get better performance in reliability and flexibility with lower cost. And in this paper, the author mainly considers two types of cluster: the one is overlapped, the other is non-overlapped. Then the author uses the mathematical expression to describe the model to let us have a clear understanding of this model.

In the description of the model, there are three important element that account for the performance of the networks, which are signal power, interference term and the achievable rate. The point we have to pay attention is that, the achievable rate means the performance. Since the interference is mainly caused by the path loss, path loss value is mainly related with the distance between the base station and user equipment, although the signal power is also associate with the distance. So, the question is with the distance increasing, is the signal power greater or the interference greater?

As for the interference term, there exists a Hurwitz zeta function [5], which is convergence and luckily, we can use the Hurwitz zeta function to express the interference term, which means the interference is convergence and limited at the same time.

After express the analytical model mathematically, we can use the expression to figure them out in MATLAB. Then, according to the figures we made out, the author optimizes the resource and power allocation, finds that there exists a situation, under such circumstances, the performance of networks is best. Also, with decreasing the distance between base stations or user equipment, the achievable rate convergence to a certain number instead of infinite.

Chapter 3: Design and Implementation

Normally there will be a part about the design and implementation of the system, especially for an implementation project. However, every project has its unique phases so you should talk to your supervisor about it.

3.1 System model

In this section, we describe the network analytical model. First of all, since the model is two dimensions, so I plot this figure like Figure 1. After this, I make the mathematical expression of model. Since the model is periodic, so we could just express one of them in both base stations and user equipment. By getting this, we are able to get the expression of path loss value. Finally, according to the path loss value, the signal power and interference term is deduced. And, what is known to all of us is that the Shannon equation could be got from both of the signal power and interference term.

we provide a detailed description of the network deployment. Second, the resource and power allocation models are explained, which feature certain spatial periodicity. Third, an expression for the achievable rates is derived from the resource and power allocation models. Finally, the function is invoked to describe the infinite source of interference.

3.1.1 Deployment description

We consider a network composed of infinite BSs that transmit to infinite UEs. Both are uniformly distributed in 2 parallel layers separated h meters, that is 2 dimensions. Therefore, the minimum distance between and BS-UE pair is h. And we consider that there are two mutually perpendicular coordinate axes, one x-axis and one y-axis in both layers. The inter-UE distance along the x-axis is d_{U_x} along the y-axis is d_{U_y}. The inter-BS distance along the x-axis is d_{B_x}, along the y-axis is d_{B_y}. We assume that the network presents certain spatial periodicity, so that $\frac{d_{B_x}}{d_{U_x}} \in \mathbb{Q}^+$, $\frac{d_{B_y}}{d_{U_y}} \in \mathbb{Q}^+$ i.e.,

$$M_x d_{U_x} = K_x d_{B_x}, \quad M_y d_{U_y} = K_y d_{B_y}, \quad M_x \in \mathbb{N}^+, M_y \in \mathbb{N}^+, K_x \in \mathbb{N}^+, K_y \in \mathbb{N}^+ . \tag{1}$$

As point out later, the equality in (1), with $M_x, M_y, K_x,$ and K_y natural numbers, ensures that the structure of the network is repeated every M_x UEs or K_x BSs along x-axis and every M_y

UEs or K_y BSs along y-axis. The location or position of a BS along the x-axis of $k_x - th$ BS is $l_{B_x}(k_x) = k_x d_{B_x}$, $k_x \in \mathbb{Z}$, the location or position of a BS along the y-axis of $k_y - th$ BS is $l_{B_y}(k_y) = k_y d_{B_y}$, $k_y \in \mathbb{Z}$, so the location or position of a BS is $l_B(k_x, k_y) = (k_x d_{B_x}, k_y d_{B_y}), k_x \in \mathbb{Z}, k_y \in \mathbb{Z}$. The location or position of a UE along the x-axis of $m_x - th$ UE is $l_{U_x}(m_x, s_x) = (m_x d_{U_x} + s_x)$, $m_x \in \mathbb{Z}$, the location or position of a BS along the y-axis of $m_y - th$ UE is $l_{U_y}(m_y, s_y) = (m_y d_{U_y} + s_y)$, $m_y \in \mathbb{Z}$.And the location of the $m_x - th$ along the x- axis with $m_y - th$ along the y-axis UE is $l_U(m_x, m_y, s_x, s_y) = (m_x d_{U_x} + s_x, m_y d_{U_y} + s_y), m_x \in \mathbb{Z}, m_y \in \mathbb{Z}$, where (s_x, s_y) is the location of UE (0,0). The structure of the system makes the only values in an area of $(0,0),(d_{U_x},0),(d_{U_x},d_{U_y}),(0,d_{U_y})$ are meaningful to (s_x, s_y). In particular, we have that $l_U(m_x, m_y, s_x, s_y) = l_U(m_x - 1, m_y - 1, s_x + d_{U_x}, s_y + d_{U_y})$, and hence the case $(s_x, s_y) = (0,0)$ and $(s_x, s_y) = (d_{U_x}, d_{U_y})$ are equivalent except for relabelling of the UEs. Hereinafter, we take $s_x \in [0, d_{U_x}]$ and $s_y \in [0, d_{U_y}]$ without loss of generality. In order to compute the expectation of the performance metrics, we assume that the location of UE (1,1)-st is uniformly distributed in the square of $(0,0),(d_{U_x},0),(d_{U_x},d_{U_y}),(0,d_{U_y})$.

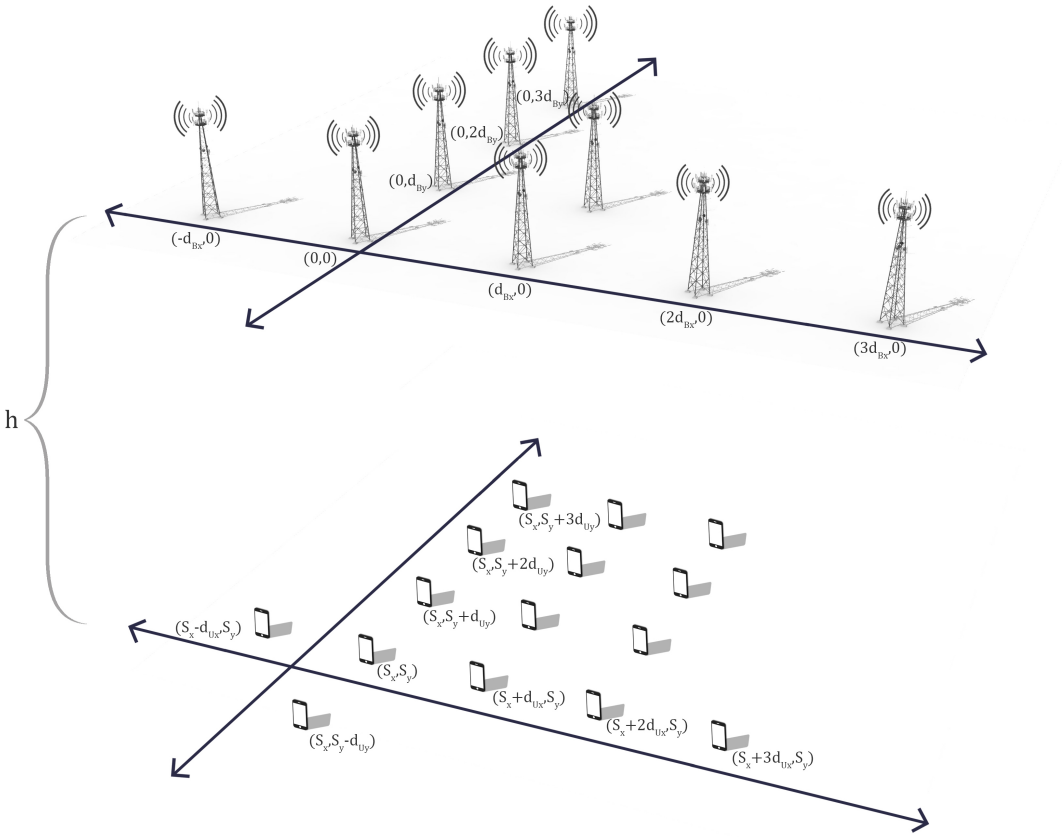

Figure 1 Two-dimensional ultra-dense network analytical model

Remark 1. Any two UEs separated a distance both greater than or equal to $M_x d_{U_x}$ in x-axis and greater than or equal to $M_y d_{U_y}$ in y-axis are served by clusters without common BSs.

In order to be able to use the Hurwitz zeta function in 2-D, path loss is computed considering 1-norm distance. In particular, the distance between $(k_x,k_y)-th$ BS and $(m_x,m_y)-th$ UE is $h+|l_{B_x}(k_x)-l_{U_x}(m_x,s_x)|+|l_{B_y}(k_y)-l_{U_y}(m_y,s_y)|$, and hence, the path loss from this BS to this UE is :

$$L_{k_x,k_y,m_x,m_y}(s_x,s_y)=(h+|l_{B_x}(k_x)-l_{U_x}(m_x,s_x)|+|l_{B_y}(k_y)-l_{U_y}(m_y,s_y)|)^{\gamma} \quad (2)$$

where γ is path loss exponent. Using Equation (1), it can be shown that

$$L_{(iK_x+k_x),(jK_y+k_y),(iM_x+m_x),(jM_y+m_y)}(s_x,s_y) = L_{k_x,k_y,m_x,m_y}(s_x,s_y) \quad (3)$$

Remark 2. The system viewed by UEs in $\{(iM_x+m_x)(jM_y+m_y)\}_{i\in\mathbb{Z},j\in\mathbb{Z}}, m_x=1,...,M_x, m_y=1,...,M_y$, is equivalent, which is also true for BSs in $\{(iK_x+k_x)(jK_y+k_y)\}_{i\in\mathbb{Z},j\in\mathbb{Z}}, k_x=1,...,K_x, k_y=1,...,K_y$.

In other words, except for the UE labelling, it is not possible to distinguish between UEs in

$\{(iM_x+m_x)(jM_y+m_y)\}_{i\in\mathbb{Z},j\in\mathbb{Z}}, m_x=1,...,M_x, m_y=1,...,M_y$

Sometimes similar occurs for BSs in

$\{(iK_x+k_x)(jK_y+k_y)\}_{i\in\mathbb{Z},j\in\mathbb{Z}}, k_x=1,...,K_x, k_y=1,...,K_y$

3.1.2 Resource and power allocation models

In this section, we will use the deployment pointed out in Remark 2 to show that the resource and power allocated in the BSs to transmit to the UEs are spatially repeated, with periodicity given by M_x, M_y, K_x, K_y. We will, then, use this fact to represent the amount of resources and power levels used for each BS-UE link with two finite-dimensional variables.

Regarding the power allocation, we assume that the transmit power is limited in each resource element to the same maximum value P. Letting $\rho_{k_x,k_y,m_x,m_y} \in [0,1]$ be the portion of the maximum power that is used by BS $(k_x,k_y)-th$ to transmit to UE $(m_x,m_y)-th$. Using Remark 2 and following a similar rational as before, we conclude that the power allocation is periodic, with the same periodicity as the resource allocation, i.e.,

$$\rho_{k_x,k_y,m_x,m_y} = \rho_{(iK_x+k_x),(jK_y+k_y),(iM_x+m_x),(jM_y+m_y)}, \forall i,j,k_x,k_y,m_x,m_y \in \mathbb{Z} \quad (4)$$

Since BSs that are not included in the cluster that serves UE $(m_x,m_y)-th$ do not spend power to transmit to this UE, we have that,

$$\rho_{(\lambda_{m_x}(s_x)+k_x),(\lambda_{m_y}(s_y)+k_y),m_x,m_y} = 0, \forall k_x \in \mathbb{Z}\setminus\{1,...,K_x\}, \forall k_y \in \mathbb{Z}\setminus\{1,...,K_y\}, \forall m_x,m_y \in \mathbb{Z} \quad (5)$$

where $((\lambda_{m_x}(s_x)+k_x),(\lambda_{m_y}(s_y)+k_y))-th$ is the left and bottom BS that serves UE $(m_x,m_y)-th$

when this UE is located at $l_U(m_x, m_y, s_x, s_y)$. Using (4) and (5), the set of all power allocations $\{\{\rho_{k_x,k_y,m_x,m_y}\}_{k_x,k_y\in\mathbb{Z}}\}_{m_x,m_y\in\mathbb{Z}}$ can be expressed by means of a matrix $X \in [0,1]^{K_x\times K_y\times M_x\times M_y}$. In particular, given certain power allocation, the (k_x, k_y, m_x, m_y) element of the corresponding matrix X, $x_{k_x k_y m_x m_y}$, is given by,

$$x_{k_x,k_y,m_x,m_y} = \rho_{((\lambda_{m_x}(s_x)+k_x),(\lambda_{m_y}(s_y)+k_y)),m_x,m_y} \tag{6}$$

and, letting $\overline{m_x} = (m-1 \bmod M_x)+1, \overline{m_y} = (m-1 \bmod M_y)+1$, the power allocation corresponding to some given matrix X is

$$\rho_{k_x,k_y,m_x,m_y} = x_{(k_x-\lambda_{m_x}(s_x)),(k_y-\lambda_{m_y}(s_y)),\overline{m_x},\overline{m_y}}$$

$$\rho_{k_x,k_y,m_x,m_y} = 0, otherwise$$

for all $k_x, k_y, m_x, m_y \in \mathbb{Z}$ (7)

3.1.3 Achievable rates

Matrix X can be used to obtain the signal and interference powers at each UE, which, at the same time, can be used to describe an achievable rate per resource element of the UEs. To this aim, we define the function:

$$p_{m_x,m_y}(y,s_x,s_y) = P\sum_{k_x=1}^{K_x}\sum_{k_y=1}^{K_y} L^{-1}_{(\lambda_{m_x}(s_x)+k_x),(\lambda_{m_y}(s_y)+k_y),m_x,m_y}(s_x,s_y)y_{k_x k_y} \tag{8}$$

$$z_{m_x m_y}(y,s_x,s_y) = P\sum_{j=-\infty}^{\infty}\sum_{i=-\infty}^{\infty}\sum_{k_x=1}^{K_x}\sum_{k_y=1}^{K_y} L^{-1}_{(\lambda_{m_x}(s_x))+iK_x+k_x),(\lambda_{m_y}(s_y))+jK_y+k_y),m_x,m_y}(s_x,s_y)y_{k_x k_y}$$
$$-P\sum_{k_x=1}^{K_x}\sum_{k_y=1}^{K_y} L^{-1}_{(\lambda_{m_x}(s_x)+k_x),(\lambda_{m_y}(s_y)+k_y),m_x,m_y}(s_x,s_y)y_{k_x k_y} \tag{9}$$

$$r_{m_x m_y}(y,s_x,s_y) = B\log(1+\frac{p_{m_x m_y}(y,s_x,s_y)}{N+z_{m_x m_y}(y,s_x,s_y)}) \tag{10}$$

Where B is a constant that accounts for the effects of the resource element bandwidth and multiple antennas, and N is the experienced noise power. The expression in (8), (9), and (10) will be used to describe the signal power, the interference power and the achievable rate,

respectively. We will do this extracting the elements of the vector y, which are the portions of the maximum power used for transmission, from the matrix X.

Letting x_{m_x} be the $m_x - th$ column of X, and letting x_{m_y} be the $m_y - th$ column of X, the signal power received by the $(m_x, m_y) - th$ UE in each resource element allocated to it is $p_{m_x m_y}(x_{\overline{m_x}}, x_{\overline{m_y}}, s_x, s_y)$. Note that, for $m_x \in \{1,...,M_x\}, m_y \in \{1,...,M_y\}$ this is equivalent to $p_{m_x m_y}(x_{m_x}, x_{m_y}, s_x, s_y)$ Due to the spatial periodicity of the system structure pointed out in Remark 2, the same signal power is received every M_x UEs along the x-axis, and every M_y along the y-axis UEs. In other words, using (3) and (4), it can be shown that

$$p_{m_x m_y}(x_{\overline{m_x}}, x_{\overline{m_y}}, s_x, s_y) = p_{\overline{m_x}\,\overline{m_y}}(x_{\overline{m_x}}, x_{\overline{m_y}}, s_x, s_y) \tag{11}$$

With respect to the interference, its power receives by the $(m_x - th, m_y - th)$ UE is $z_{m_x m_y}(x_{\overline{m_x}}, x_{\overline{m_y}}, s_x, s_y)$,which depends only on $x_{\overline{m_x}}$ and $x_{\overline{m_y}}$, and no other columns of X, due to the resource and power allocation models. Similarly, to the signal power and due to Remark 2, the same interference power is received every $M_x * M_y$ UEs, i.e.,

$$z_{m_x m_y}(x_{\overline{m_x}}, x_{\overline{m_y}}, s_x, s_y) = z_{\overline{m_x m_y}}(x_{\overline{m_x}}, x_{\overline{m_y}}, s_x, s_y) \tag{12}$$

Using the previous signal and interference levels, an achievable rate of the $(m_x - th, m_y - th)$ UE in a particular resource element is $r_{m_x m_y}(x_{\overline{m_x}}, x_{\overline{m_y}}, s_x, s_y)$. From (11) and (12), it is straightforward to show that the achievable rates are repeated every $M_x \times M_y$ UEs, i.e.,

$$r_{m_x m_y}(x_{\overline{m_x}}, x_{\overline{m_y}}, s_x, s_y) = r_{\overline{m_x m_y}}(x_{\overline{m_x}}, x_{\overline{m_y}}, s_x, s_y) \tag{13}$$

The total achievable rate of the $M_x \times M_y$ UE is a multiple of $r_{m_x m_y}(x_{\overline{m_x}}, x_{\overline{m_y}}, s_x, s_y)$ that depends on the amount of resource elements allocated to the UE. Defining the function

$$R_{m_x m_y}(\upsilon, y, s_x, s_y) = W \upsilon r_{m_x m_y}(y, s_x, s_y) \tag{14}$$

this rate can be expressed as $R_{m_x m_y}(\omega_{\overline{m_x}\,\overline{m_y}}, x_{\overline{m_x}\,\overline{m_y}}, s_x, s_y)$

3.1.4 Convergence of the interference term

In the 2-dimensional deployment, in which infinite UEs and BSs are homogeneously distributed in two dimensions. In this case, the interference can be modelled as a double series whose convergence point can be expressed using also the Barnes zeta function. In particular, the

$\zeta_N(s,w|a_1,...,a_N)=\sum_{m_1,...,m_N=0}^{\infty}(w+m_1a_1+...+m_Na_N)^{-s}$ converges for all $s>N$, $w>0$ and $a_1,...,a_N>0$.

In this case, the interference power

$$z_{m_x m_y}(y,s_x,s_y)=P\sum_{j=-\infty}^{\infty}\sum_{i=-\infty}^{\infty}\sum_{k_x=1}^{K_x}\sum_{k_y=1}^{K_y}L^{-1}_{(\lambda_{m_x}(s_x))+iK_x+k_x),(\lambda_{m_y}(s_y))+jK_y+k_y),m_x,m_y}(s_x,s_y)y_{k_xk_y}$$

$$-P\sum_{k_x=1}^{K_x}\sum_{k_y=1}^{K_y}L^{-1}_{(\lambda_{m_x}(s_x)+k_x),(\lambda_{m_y}(s_y)+k_y),m_x,m_y}(s_x,s_y)y_{k_xk_y}$$

can be expressed as

$$z_{m_xm_y}(y,s_x,s_y)=$$

$$P\sum_{j=-\infty}^{\infty}\sum_{i=-\infty}^{\infty}\sum_{k_x=1}^{K_x}\sum_{k_y=1}^{K_y}(h+|(\lambda_{m_x}(s_x)+iK_x+k_x)d_{B_x}-m_xd_{U_x}-s_x|+|(\lambda_{m_y}(s_y)+jK_y+k_y)d_{B_y}-m_yd_{U_y}-s_y|)^{-\gamma}y_{k_xk_y}$$

$$-P\sum_{k_x=1}^{K_x}\sum_{k_y=1}^{K_y}(h+|(\lambda_{m_x}(s_x)+k_x)d_{B_x}-m_xd_{U_x}-s_x|+|(\lambda_{m_y}(s_y)+k_y)d_{B_y}-m_yd_{U_y}-s_y|)^{-\gamma}(s_x,s_y)y_{k_xk_y} \quad (15)$$

$$=P\sum_{j'=1}^{\infty}\sum_{i'=1}^{\infty}\sum_{k_x=1}^{K_x}\sum_{k_y=1}^{K_y}(h+|(\lambda_{m_x}(s_x)+i'K_x+k_x)d_{B_x}-m_xd_{U_x}-s_x|+|(\lambda_{m_y}(s_y)+j'K_y+k_y)d_{B_y}-m_yd_{U_y}-s_y|)^{-\gamma}(s_x,s_y)y_{k_xk_y} \quad (16)$$

$$+P\sum_{i'=1}^{\infty}\sum_{k_x=1}^{K_x}\sum_{k_y=1}^{K_y}(h+|(\lambda_{m_x}(s_x)+i'K_x+k_x)d_{B_x}-m_xd_{U_x}-s_x|+|(\lambda_{m_y}(s_y)+k_y)d_{B_y}-m_yd_{U_y}-s_y|)^{-\gamma}(s_x,s_y)y_{k_xk_y} \quad (17)$$

$$+P\sum_{j'=-\infty}^{-1}\sum_{i'=1}^{\infty}\sum_{k_x=1}^{K_x}\sum_{k_y=1}^{K_y}(h+|(\lambda_{m_x}(s_x)+i'K_x+k_x)d_{B_x}-m_xd_{U_x}-s_x|+|(\lambda_{m_y}(s_y)+j'K_y+k_y)d_{B_y}-m_yd_{U_y}-s_y|)^{-\gamma}(s_x,s_y)y_{k_xk_y} \quad (18)$$

$$+P\sum_{j'=-\infty}^{-1}\sum_{k_x=1}^{K_x}\sum_{k_y=1}^{K_y}(h+|(\lambda_{m_x}(s_x)+k_x)d_{B_x}-m_xd_{U_x}-s_x|+|(\lambda_{m_y}(s_y)+j'K_y+k_y)d_{B_y}-m_yd_{U_y}-s_y|)^{-\gamma}(s_x,s_y)y_{k_xk_y} \quad (19)$$

$$+P\sum_{j'=-\infty}^{-1}\sum_{i'=-\infty}^{-1}\sum_{k_x=1}^{K_x}\sum_{k_y=1}^{K_y}(h+|(\lambda_{m_x}(s_x)+i'K_x+k_x)d_{B_x}-m_xd_{U_x}-s_x|+|(\lambda_{m_y}(s_y)+j'K_y+k_y)d_{B_y}-m_yd_{U_y}-s_y|)^{-\gamma}(s_x,s_y)y_{k_xk_y} \quad (20)$$

$$+P\sum_{i'=-\infty}^{-1}\sum_{k_x=1}^{K_x}\sum_{k_y=1}^{K_y}(h+|(\lambda_{m_x}(s_x)+i'K_x+k_x)d_{B_x}-m_xd_{U_x}-s_x|+|(\lambda_{m_y}(s_y)+k_y)d_{B_y}-m_yd_{U_y}-s_y|)^{-\gamma}(s_x,s_y)y_{k_xk_y} \quad (21)$$

$$+P\sum_{j'=1}^{\infty}\sum_{i'=-\infty}^{-1}\sum_{k_x=1}^{K_x}\sum_{k_y=1}^{K_y}(h+|(\lambda_{m_x}(s_x)+i'K_x+k_x)d_{B_x}-m_xd_{U_x}-s_x|+|(\lambda_{m_y}(s_y)+j'K_y+k_y)d_{B_y}-m_yd_{U_y}-s_y|)^{-\gamma}(s_x,s_y)y_{k_xk_y} \quad (22)$$

$$+P\sum_{j'=1}^{\infty}\sum_{k_x=1}^{K_x}\sum_{k_y=1}^{K_y}(h+|(\lambda_{m_x}(s_x)+k_x)d_{B_x}-m_xd_{U_x}-s_x|+|(\lambda_{m_y}(s_y)+j'K_y+k_y)d_{B_y}-m_yd_{U_y}-s_y|)^{-\gamma}(s_x,s_y)y_{k_xk_y} \quad (23)$$

Let us take (16) as an example. Firstly, let $i=i'-1, j=j'-1$, so

$$=P\sum_{j'=1}^{\infty}\sum_{i'=1}^{\infty}\sum_{k_x=1}^{K_x}\sum_{k_y=1}^{K_y}(h+|(\lambda_{m_x}(s_x)+i'K_x+k_x)d_{B_x}-m_xd_{U_x}-s_x|+|(\lambda_{m_y}(s_y)+j'K_y+k_y)d_{B_y}-m_yd_{U_y}-s_y|)^{-\gamma}(s_x,s_y)y_{k_xk_y} \quad (24)$$

will become

$$=P\sum_{j=0}^{\infty}\sum_{i=0}^{\infty}\sum_{k_x=1}^{K_x}\sum_{k_y=1}^{K_y}[h+(\lambda_{m_x}(s_x)+(i+1)K_x+k_x)d_{B_x}-m_xd_{U_x}-s_x+(\lambda_{m_y}(s_y)+(j+1)K_y+k_y)d_{B_y}-m_yd_{U_y}-s_y]^{-\gamma}y_{k_xk_y} \quad (25)$$

And according to the Barnes' multiple zeta function $\zeta_N(s,w|a_1,...,a_N)$ depends on the parameters $a_1,...,a_N$ that will be taken positive and which is defined by the series

$$\zeta_N(s,w|a_1,...,a_N)=\sum_{m_1,...,m_N=0}^{\infty}(w+m_1a_1+...+m_Na_N)^{-s} \quad (26)$$

$\mathrm{Re}\,w>0$, $\mathrm{Re}\,s>N$

So, (16) will become

$$=P\sum_{j=0}^{\infty}\sum_{i=0}^{\infty}\sum_{k_x=1}^{K_x}\sum_{k_y=1}^{K_y}[h+\lambda_{m_x}(s_x)d_{B_x}+K_xd_{B_x}+k_xd_{B_x}-m_xd_{U_x}-s_x+\lambda_{m_y}(s_y)d_{B_y}+K_yd_{B_y}+k_yd_{B_y}-m_yd_{U_y}-s_y+iK_xd_{B_x}+jK_yd_{B_y}]^{-\gamma}y_{k_xk_y}$$

$$=P\sum_{k_x=1}^{K_x}\sum_{k_y=1}^{K_y}\zeta_2(\gamma,w_1|\alpha_{11},\alpha_{12})y_{k_xk_y} \quad (27)$$

where

$$w_1=h+\lambda_{m_x}(s_x)d_{B_x}+K_xd_{B_x}+k_xd_{B_x}-m_xd_{U_x}-s_x+\lambda_{m_y}(s_y)d_{B_y}+K_yd_{B_y}+k_yd_{B_y}-m_yd_{U_y}-s_y>0 \quad (28)$$

$$\alpha_{11}=K_xd_{B_x}>0 \quad (29)$$

$$\alpha_{12}=K_yd_{B_y}>0 \quad (30)$$

$((\lambda_{m_x}(s_x)+K_x+k_x)d_{B_x},(\lambda_{m_y}(s_y)+K_y+k_y)d_{B_y})$ is the location of the $(k_x,k_y)-th$ closest interferer BS to the right and top of the cluster that serves the $(m_x,m_y)-th$ UE. Therefore, it is straightforward to show that $(\lambda_{m_x}(s_x)+K_x+k_x)d_{B_x}>m_xd_{U_x}+s_x$ and $(\lambda_{m_y}(s_y)+K_y+k_y)d_{B_y}>+m_yd_{U_y}+s_y$, which yields the inequality in (16). And this is the reason why $w_1>0$.

As for (18), let $i = i' - 1$ and $j = -j' - 1$, so

$$+P\sum_{j'=-\infty}^{-1}\sum_{i'=1}^{\infty}\sum_{k_x=1}^{K_x}\sum_{k_y=1}^{K_y}(h+|(\lambda_{m_x}(s_x)+i'K_x+k_x)d_{B_x}-m_xd_{U_x}-s_x|+|(\lambda_{m_y}(s_y)+j'K_y+k_y)d_{B_y}-m_yd_{U_y}-s_y|)^{-\gamma}(s_x,s_y)y_{k_xk_y}>0$$

will become

$$=P\sum_{k_x=1}^{K_x}\sum_{k_y=1}^{K_y}\zeta_2(\gamma,w_3\,|\,\alpha_{31},\alpha_{32})y_{k_xk_y} \tag{31}$$

where

$$w_3 = h+\lambda_{m_x}(s_x)d_{B_x}+K_xd_{B_x}+k_xd_{B_x}-m_xd_{U_x}-s_x-\lambda_{m_y}(s_y)d_{B_y}+K_yd_{B_y}-k_yd_{B_y}+m_yd_{U_y}+s_y>0 \tag{32}$$

$$\alpha_{31} = K_xd_{B_x}>0 \tag{33}$$

$$\alpha_{32} = K_yd_{B_y}>0 \tag{34}$$

As for (17), let $i = i' - 1$

$$+P\sum_{i'=1}^{\infty}\sum_{k_x=1}^{K_x}\sum_{k_y=1}^{K_y}(h+|(\lambda_{m_x}(s_x)+i'K_x+k_x)d_{B_x}-m_xd_{U_x}-s_x|+|(\lambda_{m_y}(s_y)+k_y)d_{B_y}-m_yd_{U_y}-s_y|)^{-\gamma}(s_x,s_y)y_{k_xk_y}$$

$$=P\sum_{k_x=1}^{K_x}\sum_{k_y=1}^{K_y}\sum_{i=0}^{\infty}[h+(\lambda_{m_x}(s_x)+(i+1)K_x+k_x)d_{B_x}-m_xd_{U_x}-s_x+(\lambda_{m_y}(s_y)+k_y)d_{B_y}-m_yd_{U_y}-s_y]^{-\gamma}\,y_{k_xk_y} \tag{35}$$

$$=P\sum_{k_x=1}^{K_x}\sum_{k_y=1}^{K_y}\zeta_1(\gamma,w_2\,|\,\alpha_2)y_{k_xk_y} \tag{36}$$

$$w_2 = h+(\lambda_{m_x}(s_x)+k_x+K_x)d_{B_x}-m_xd_{U_x}-s_x+|(\lambda_{m_y}(s_y)+k_y)d_{B_y}-m_yd_{U_y}-s_y|>0 \tag{37}$$

$$\alpha_2 = K_xd_{B_x}>0 \tag{38}$$

So, we can draw the conclusion that

$$z_{m_xm_y}(y,s_x,s_y)=P\sum_{j=-\infty}^{\infty}\sum_{i=-\infty}^{\infty}\sum_{k_x=1}^{K_x}\sum_{k_y=1}^{K_y}L^{-1}_{(\lambda_{m_x}(s_x))+iK_x+k_x),(\lambda_{m_y}(s_y))+jK_y+k_y),m_x,m_y}(s_x,s_y)y_{k_xk_y}$$

$$-P\sum_{k_x=1}^{K_x}\sum_{k_y=1}^{K_y}L^{-1}_{(\lambda_{m_x}(s_x)+k_x),(\lambda_{m_y}(s_y)+k_y),m_x,m_y}(s_x,s_y)y_{k_xk_y}$$

$$=P\sum_{k_x=1}^{K_x}\sum_{k_y=1}^{K_y}[\zeta_2(\gamma,w_1\,|\,\alpha_{11},\alpha_{12})+\zeta_2(\gamma,w_3\,|\,\alpha_{31},\alpha_{32})+\zeta_2(\gamma,w_5\,|\,\alpha_{51},\alpha_{52})$$

$$+\zeta_2(\gamma,w_7\,|\,\alpha_{71},\alpha_{72})+\zeta_1(\gamma,w_2\,|\,\alpha_2)+\zeta_1(\gamma,w_2\,|\,\alpha_2)+\zeta_1(\gamma,w_2\,|\,\alpha_2)+\zeta_1(\gamma,w_2\,|\,\alpha_2))]y_{k_xk_y} \tag{39}$$

Where

$$w_1 = h+\lambda_{m_x}(s_x)d_{B_x}+K_xd_{B_x}+k_xd_{B_x}-m_xd_{U_x}-s_x+\lambda_{m_y}(s_y)d_{B_y}+K_yd_{B_y}+k_yd_{B_y}-m_yd_{U_y}-s_y>0 \tag{40}$$

$$w_2 = h + (\lambda_{m_x}(s_x) + k_x + K_x)d_{B_x} - m_x d_{U_x} - s_x + |(\lambda_{m_y}(s_y) + k_y)d_{B_y} - m_y d_{U_y} - s_y| > 0 \quad (41)$$

$$w_3 = h + \lambda_{m_x}(s_x)d_{B_x} + K_x d_{B_x} + k_x d_{B_x} - m_x d_{U_x} - s_x - \lambda_{m_y}(s_y)d_{B_y} + K_y d_{B_y} - k_y d_{B_y} + m_y d_{U_y} + s_y > 0 \quad (42)$$

$$w_4 = h + |(\lambda_{m_x}(s_x) + k_x)d_{B_x} - m_x d_{U_x} - s_x| - (\lambda_{m_y}(s_y) + k_y - K_y)d_{B_y} + m_y d_{U_y} + s_y > 0 \quad (43)$$

$$w_5 = h - \lambda_{m_x}(s_x)d_{B_x} + K_x d_{B_x} - k_x d_{B_x} + m_x d_{U_x} + s_x - \lambda_{m_y}(s_y)d_{B_y} + K_y d_{B_y} - k_y d_{B_y} + m_y d_{U_y} + s_y > 0 \quad (44)$$

$$w_6 = h - (\lambda_{m_x}(s_x) + k_x - K_x)d_{B_x} + m_x d_{U_x} + s_x + |(\lambda_{m_y}(s_y) + k_y)d_{B_y} - m_y d_{U_y} - s_y| > 0 \quad (45)$$

$$w_7 = h - \lambda_{m_x}(s_x)d_{B_x} + K_x d_{B_x} - k_x d_{B_x} + m_x d_{U_x} + s_x + \lambda_{m_y}(s_y)d_{B_y} + K_y d_{B_y} + k_y d_{B_y} - m_y d_{U_y} - s_y > 0 \quad (46)$$

$$w_8 = h + |(\lambda_{m_x}(s_x) + k_x)d_{B_x} - m_x d_{U_x} - s_x| + (\lambda_{m_y}(s_y) + k_y + K_y)d_{B_y} - m_y d_{U_y} - s_y > 0 \quad (47)$$

$$\alpha_{11} = K_x d_{B_x} > 0 \quad (48)$$

$$\alpha_{12} = K_y d_{B_y} > 0 \quad (49)$$

$$\alpha_2 = K_x d_{B_x} > 0 \quad (50)$$

$$\alpha_{31} = K_x d_{B_x} > 0 \quad (51)$$

$$\alpha_{32} = K_y d_{B_y} > 0 \quad (52)$$

$$\alpha_4 = K_y d_{B_y} > 0 \quad (53)$$

$$\alpha_{51} = K_x d_{B_x} > 0 \quad (54)$$

$$\alpha_{52} = K_y d_{B_y} > 0 \quad (55)$$

$$\alpha_6 = K_x d_{B_x} > 0 \quad (56)$$

$$\alpha_{71} = K_x d_{B_x} > 0 \quad (57)$$

$$\alpha_{72} = K_y d_{B_y} > 0 \quad (58)$$

$$\alpha_8 = K_y d_{B_y} > 0 \quad (59)$$

Chapter 4: Results and Discussion

4.1 Achievable rates of UDNs

In this section, we would find out the outcomes which is come from the model in the previous section, mostly, to find out how the number of base stations in one cluster or the number of user equipment in one cluster or, especially, to figure out how the distance between base station would influence the performance of the ultra-dense networks.In particular, the behaviour of the achievable rates is evaluated with respect to the inter-BS distance $d_{B_x} + d_{B_y}$. In order to observe the effects of densification without the distortion caused by introducing more available power in dense networks, the maximum transmitted power per resource element in each BS is set to $P = \eta_x d_{B_x} + \eta_y d_{B_y}$, where η_x is the available power per meter and resource element along the x-axis and η_y is the available power per meter and resource element along the y-axis. The rates in this section were obtained with the resource and power allocation of the previous section and assuming h=B=W=N=1 and $\gamma = 3$. Note that, by selecting h=1 and N=1, P can be understood as the maximum signal to noise (SNR) of any BS-UE link.

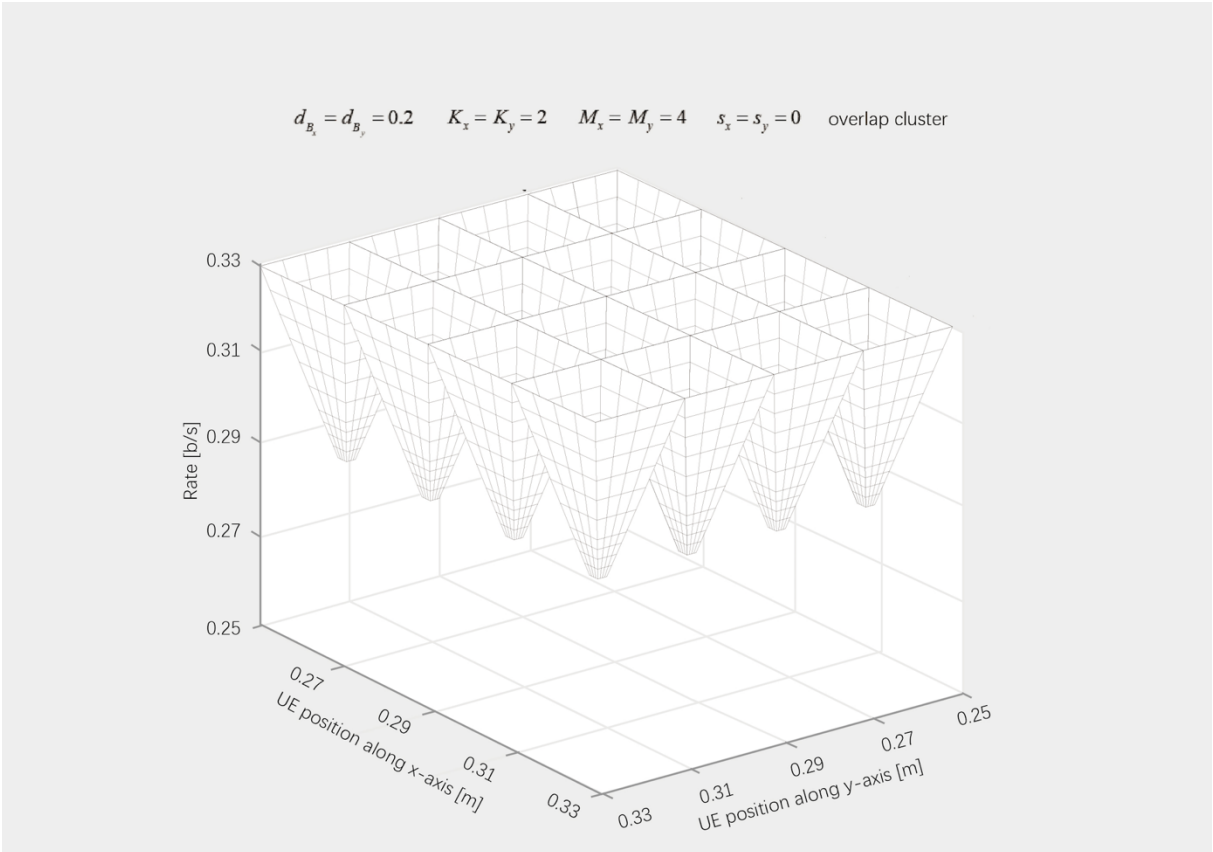

Figure 2 achievable rates with respect to the UEs position for different inter-BS distances and clustering types.

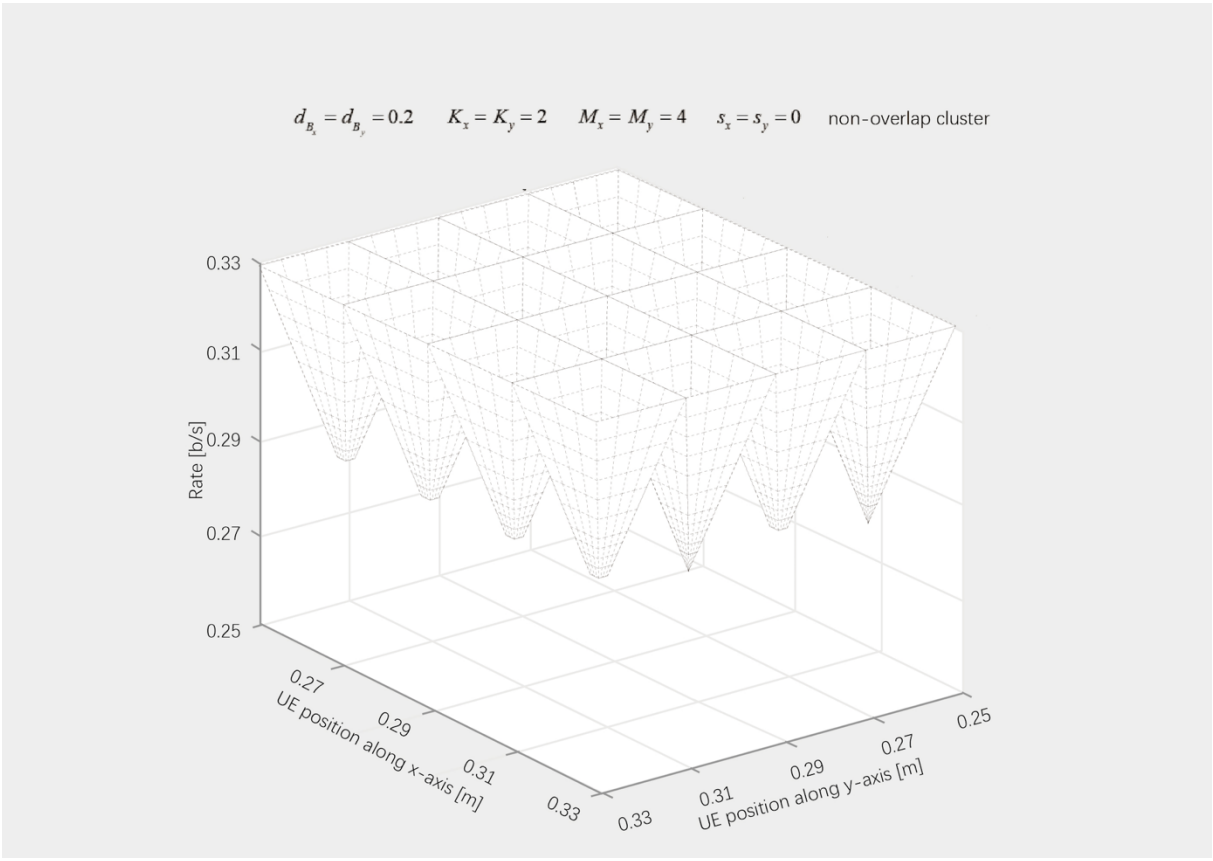

Figure 3 achievable rates with respect to the UEs position for different inter-BS distances and clustering types.

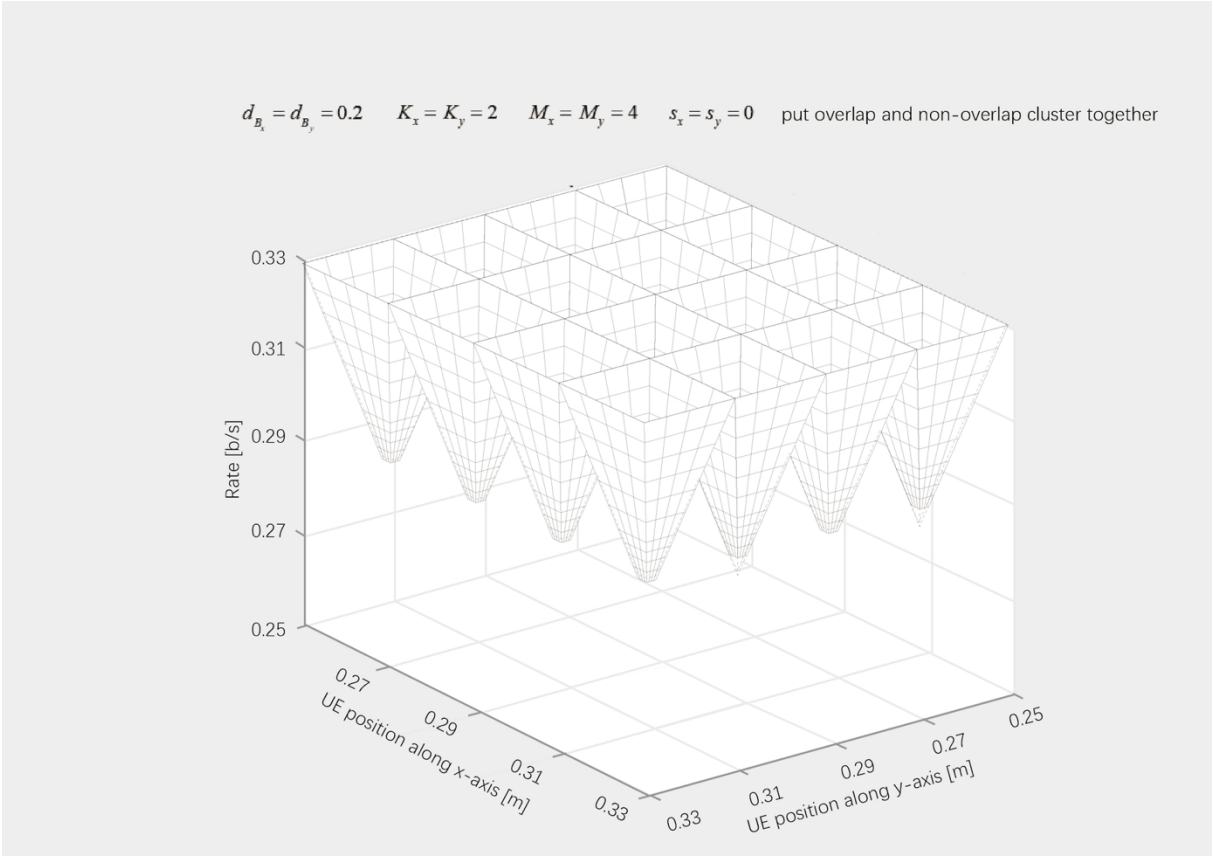

Figure 4 achievable rates with respect to the UEs position for different inter-BS distances and clustering types.

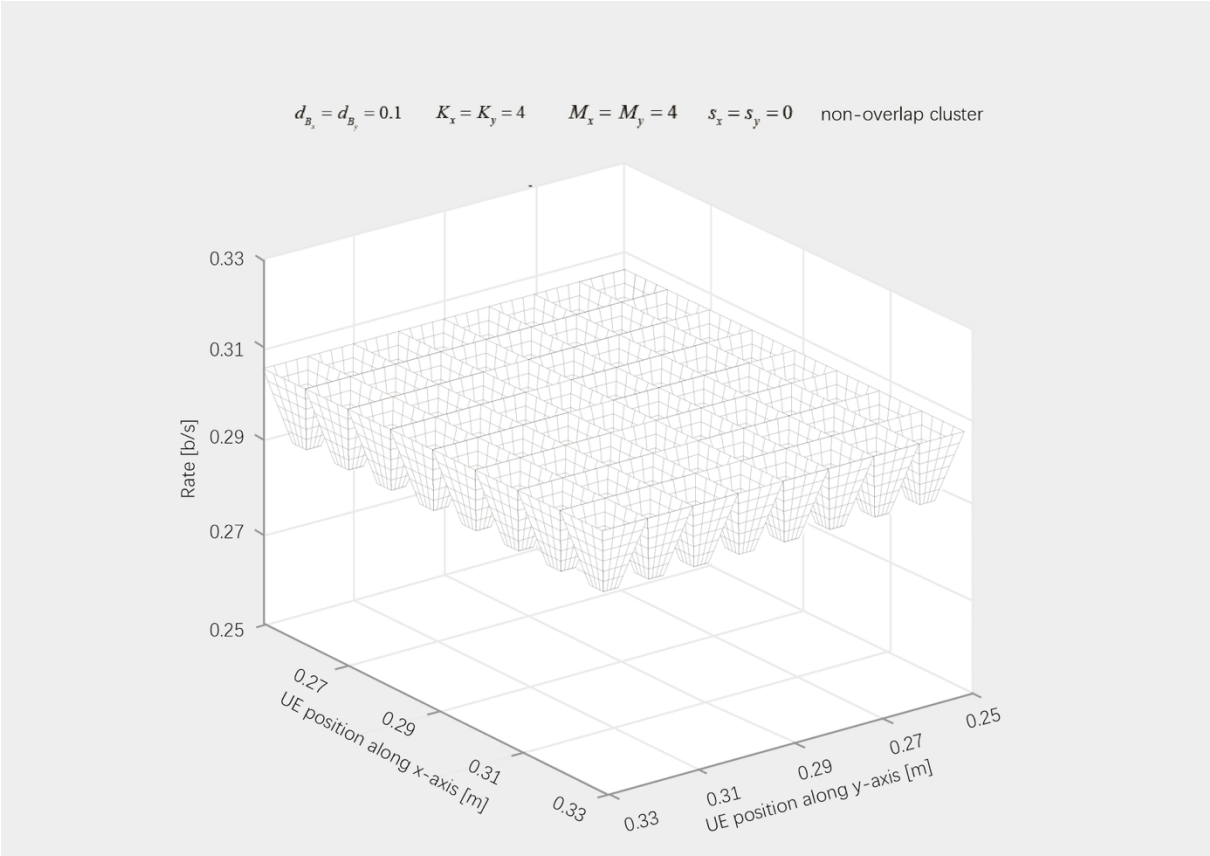

Figure 5 achievable rates with respect to the UEs position for different inter-BS distances and clustering types.

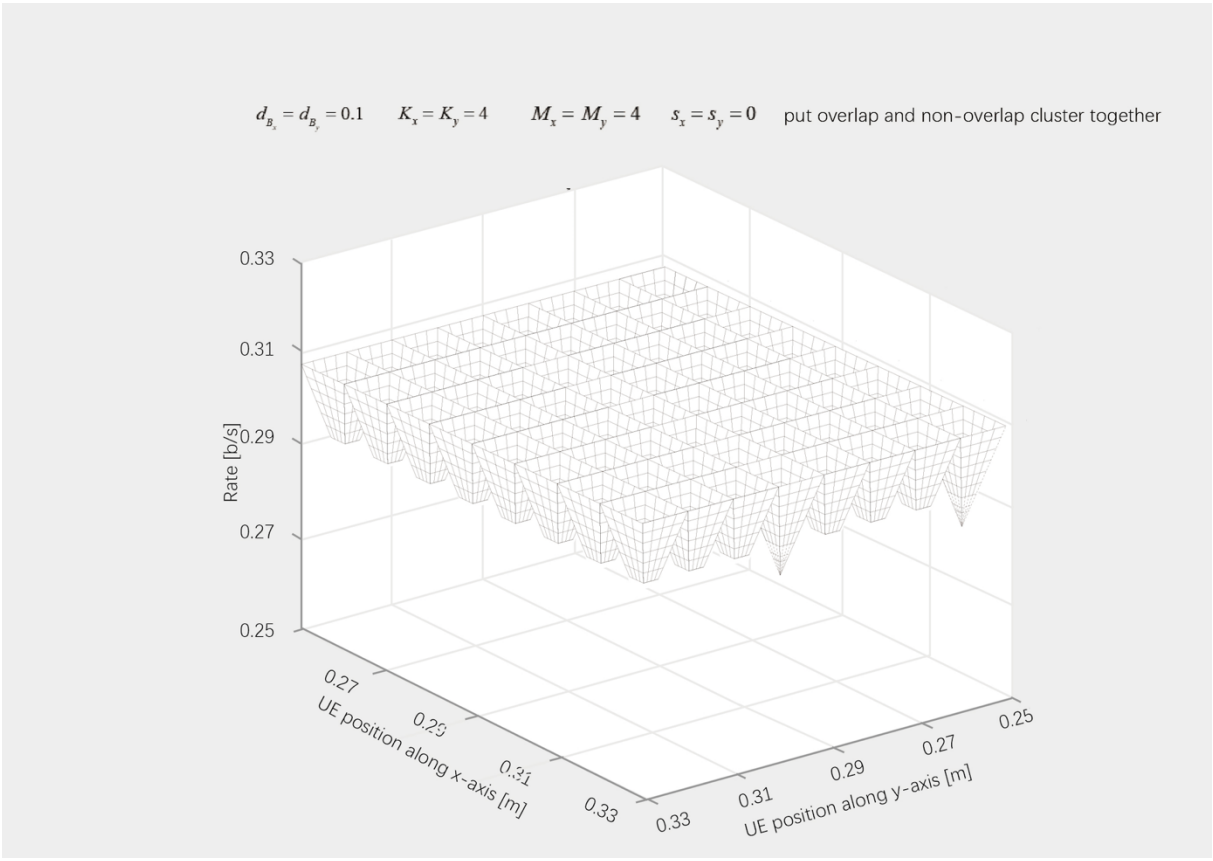

Figure 6 achievable rates with respect to the UEs position for different inter-BS distances and clustering types.

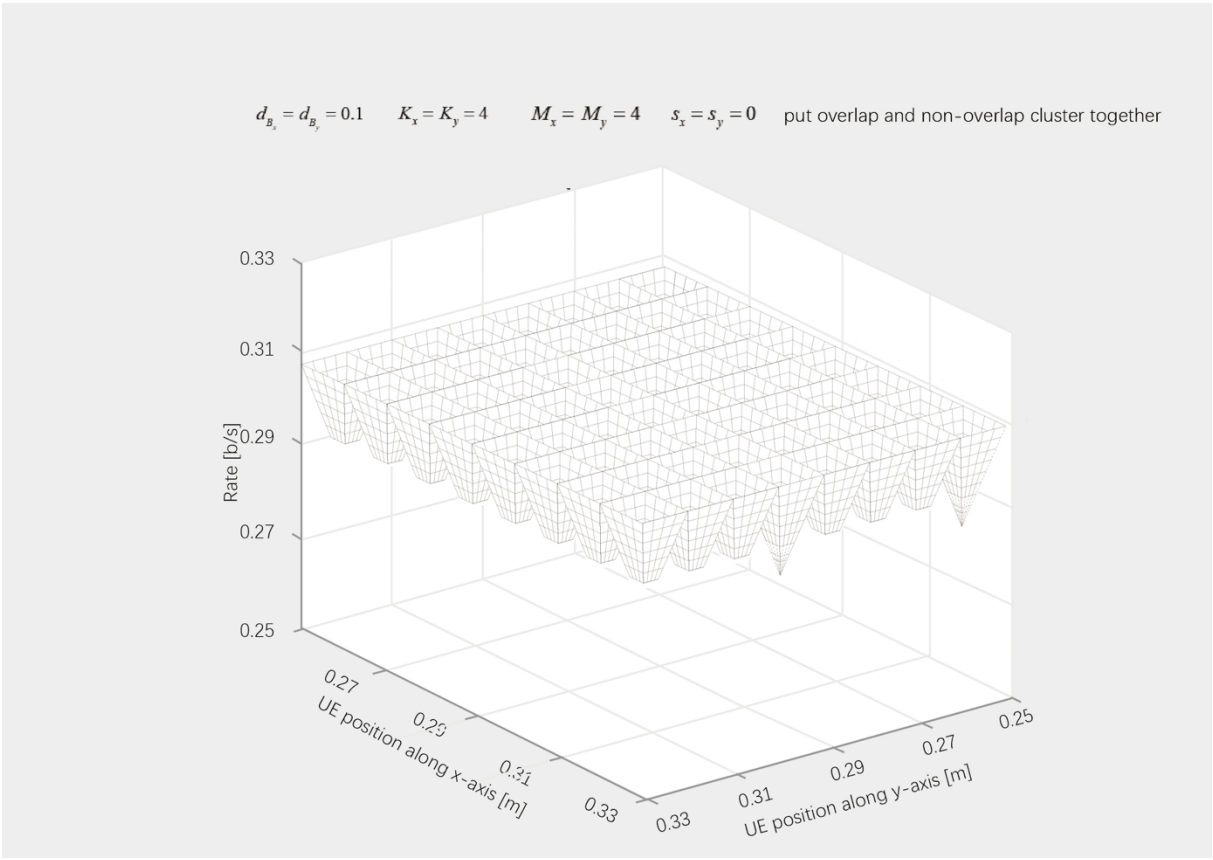

Figure 7 achievable rates with respect to the UEs position for different inter-BS distances and clustering types.

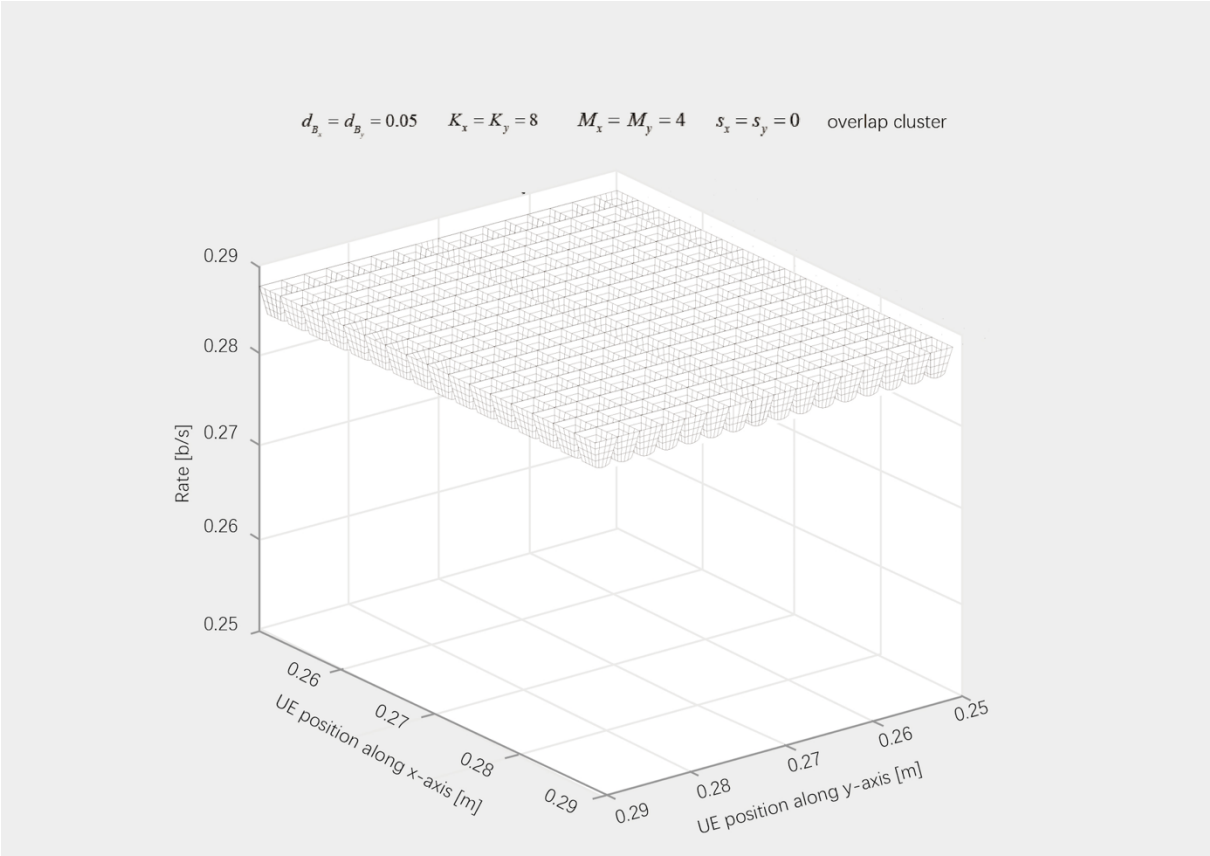

Figure 8 achievable rates with respect to the UEs position for different inter-BS distances and clustering types.

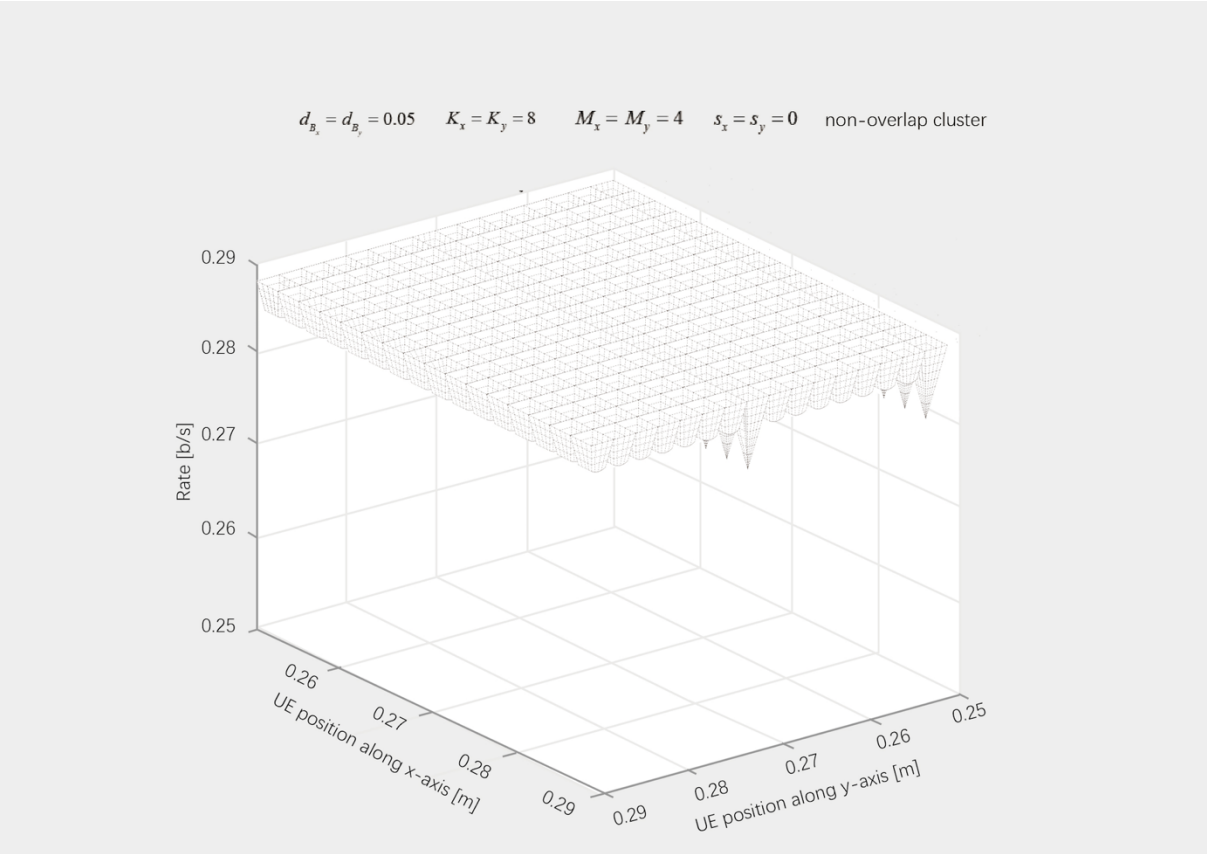

Figure 9 achievable rates with respect to the UEs position for different inter-BS distances and clustering types.

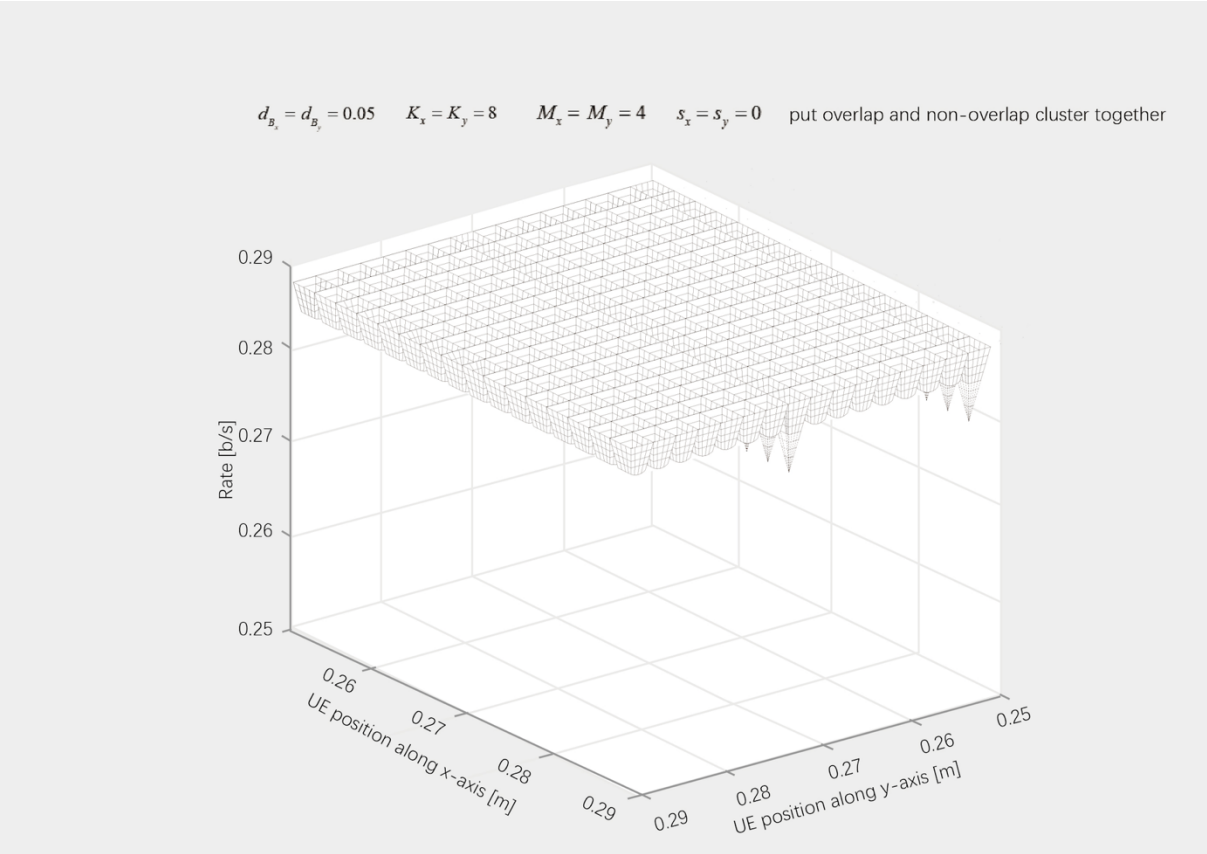

Figure 10 achievable rates with respect to the UEs position for different inter-BS distances and clustering types.

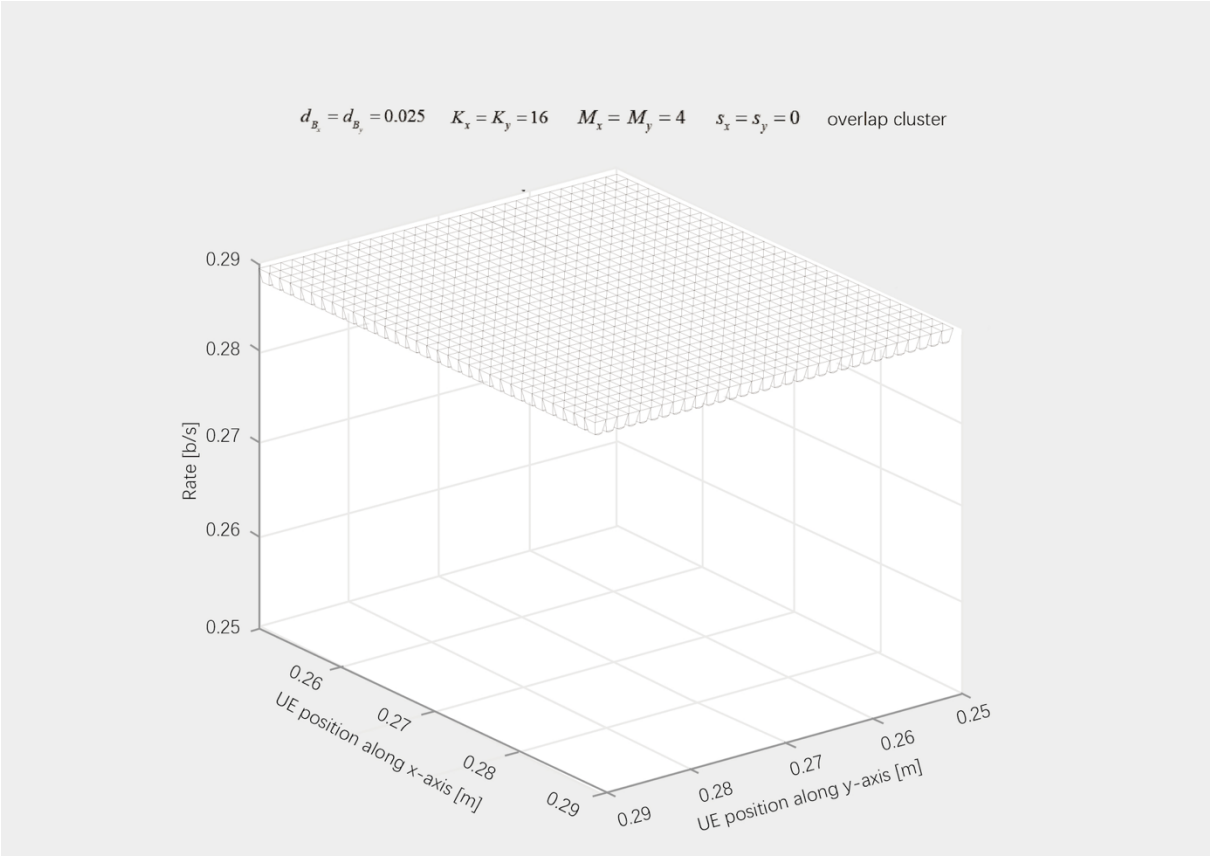

Figure 11 achievable rates with respect to the UEs position for different inter-BS distances and clustering types.

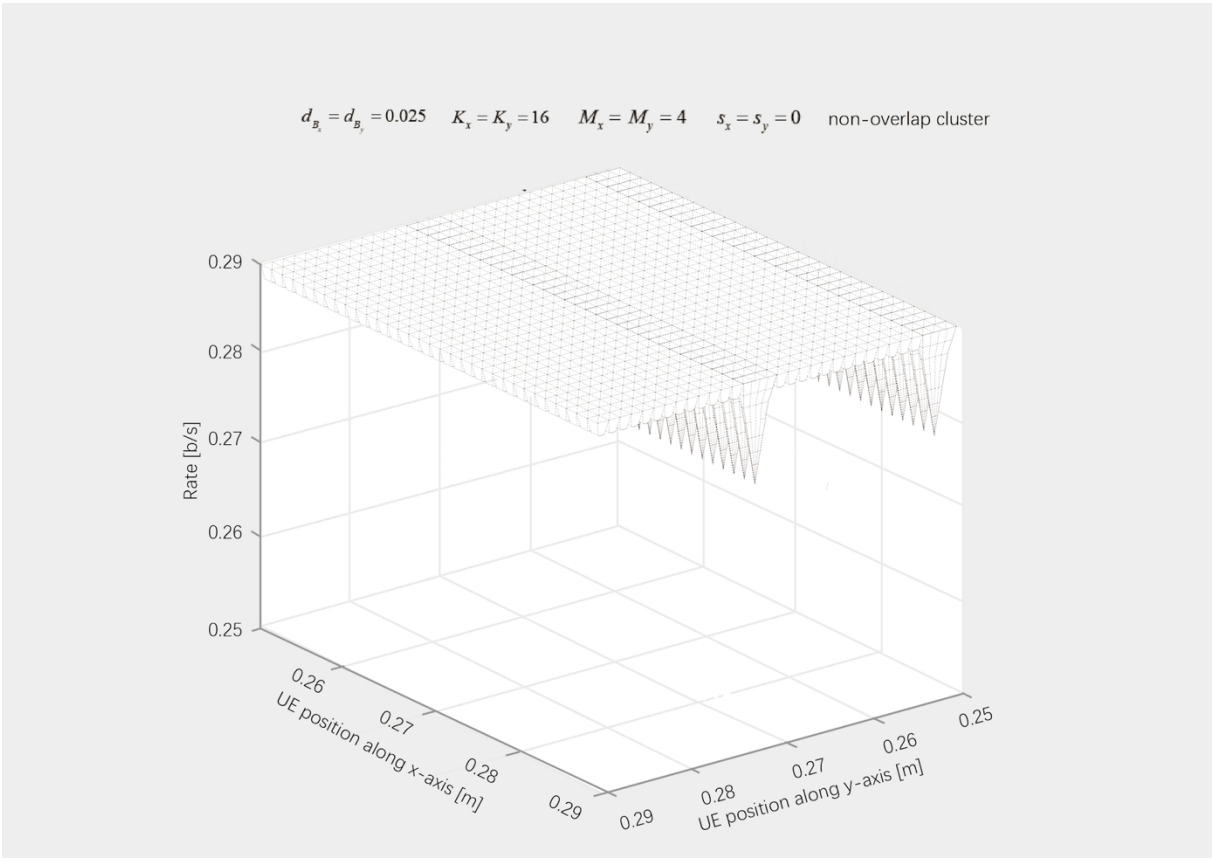

Figure 12 achievable rates with respect to the UEs position for different inter-BS distances and clustering types1.

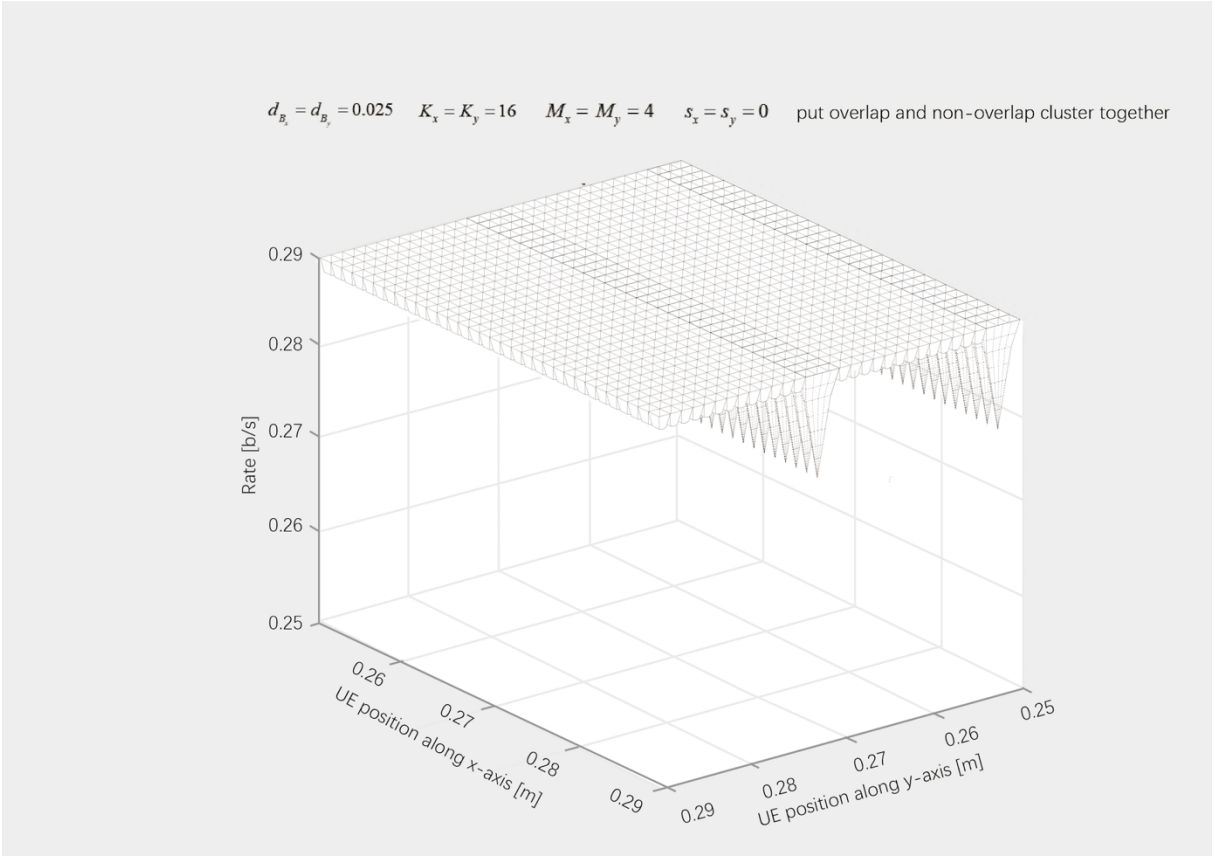

Figure 13 achievable rates with respect to the UEs position for different inter-BS distances and clustering types.

Figure 2-13 shows the achievable rates with respect to the UEs location or position in the x-axis and y-axis for four different inter-BS distances and two clustering techniques: overlapped and no overlapped clustering. The four figures were obtained setting $d_{U_x} = d_{U_y} = 0.1$ $\eta_x = \eta_y = 100$ and $M_x = M_y = 4$, and varying the values of $d_{B_x}, d_{B_y}, K_x, K_y$. Specifically, we set $d_{B_x} = d_{B_y} = 0.2$ and $K_x = K_y = 2$ in Figure 2,3,4,5, and $d_{B_x} = d_{B_y} = 0.1$ and $K_x = K_y = 4$ in Figure 5,6,7. Figure 2-13 show that, in all studies cases, since we could find that the overlapped ones always greater or equal to those with the non-overlapped clusters in the achievable rate. The difference between these two techniques are especially significant around the cluster borders and in denser networks. Note, for instance, the significant rate drops around the position exhibited by the non-overlapped clusters in Figure 11,12,13. Near the cluster centre, both clustering techniques have a very similar behaviour.

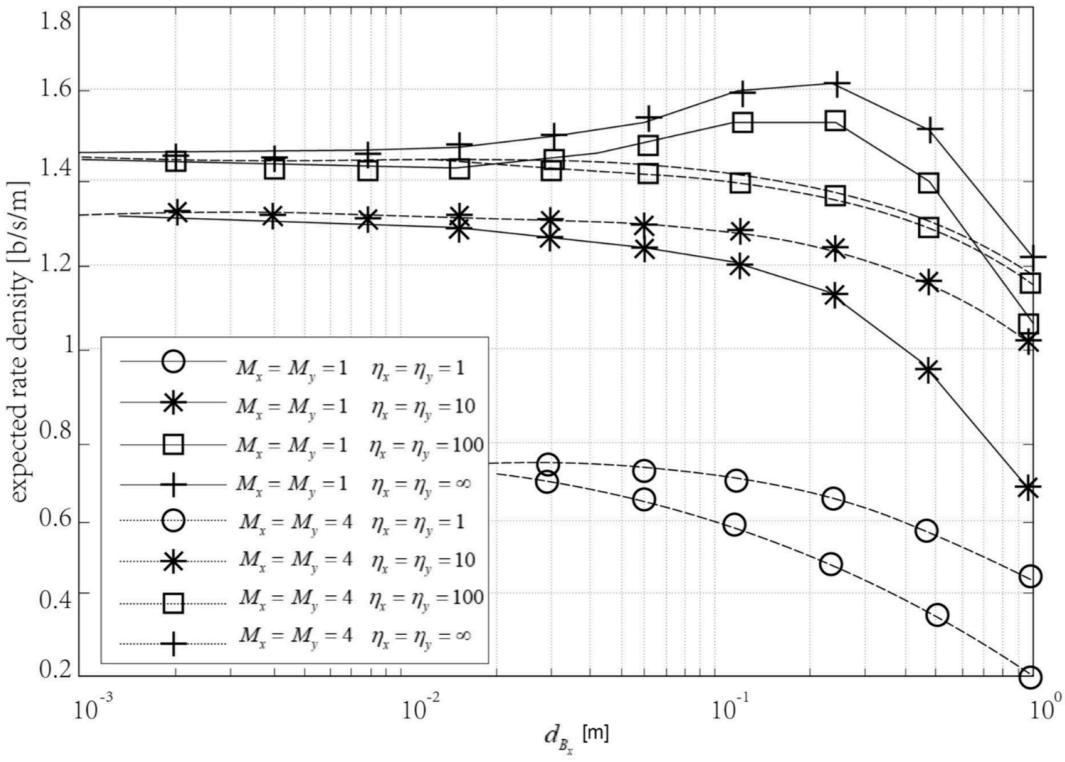

Figure 14 Expected rate density versus BS density for different values of available power meter.

It is important to note that, in Figure 14, the rate with overlapped clusters seems to converge to some value in the interval when $d_{B_x} \to 0$ and $d_{B_y} \to 0$, which contradicts the conclusion in [6], [7], i.e., rate increases linearly with along the x-axis or y-axis with BS density. This conclusion was obtained in [6], [7] by considering lack of cooperation among BSs and deployments with more UEs than BSs. Due to this, resources were shared among less UEs by increasing the quantity of BSs, which, together with the SINE invariance, led these works to conclude that the achievable rate should increase linearly along the x-axis or y-axis with BS density. However, in the particular case of Figure 14, UE density is constant and resources are shared among $M_x = M_y = 4$. The fact that the rate converges implies that the SINR also converges, supporting some kind of SINR invariance as observed in [6], [7], but noting that this is not always accompanied by a rate increment.

The SINR invariance was refuted in [8], [9] using the dual-slope path loss model. However, this is not uniquely caused by the particular characteristics of this model. We will show that the same conclusion can be achieved with our system and path loss models by increasing both UE and BS density. To this aim, we computed an average metric of the achievable rates similar to the system throughput obtained in [8], [9]. In particular, the metric was the expected rate density, i.e., the expected rate provided by the network per meter, where expectation is taken over (s_x, s_y) uniformly distributed in the area of $(0,0),(d_{U_x},0),(d_{U_x},d_{U_y}),(0,d_{U_y})$, that is

$$E_R = E[\frac{1}{M_x d_{U_x} + M_y d_{U_y}} \sum_{m_x=1}^{M_x} \sum_{m_y=1}^{M_y} R_{m_x,m_y}(\omega_{m_x,m_y}*(s_x,s_y), x_{m_x,m_y}*(s_x,s_y), s_x, s_y)]$$

$$= \frac{1}{M_x d_{U_x}^2 + M_x d_{U_x}^2} \int_0^{d_{U_x}} \int_0^{d_{U_y}} \sum_{m_x=1}^{M_x} \sum_{m_y=1}^{M_y} R_{m_x,m_y}(\omega_{m_x,m_y}*(s_x,s_y), x_{m_x,m_y}*(s_x,s_y), s_x, s_y) ds_x ds_y \quad (59)$$

The results of the rest of this section were obtained for only overlapped clustering technique, due to its superior performance in comparison with non-overlapped clusters.

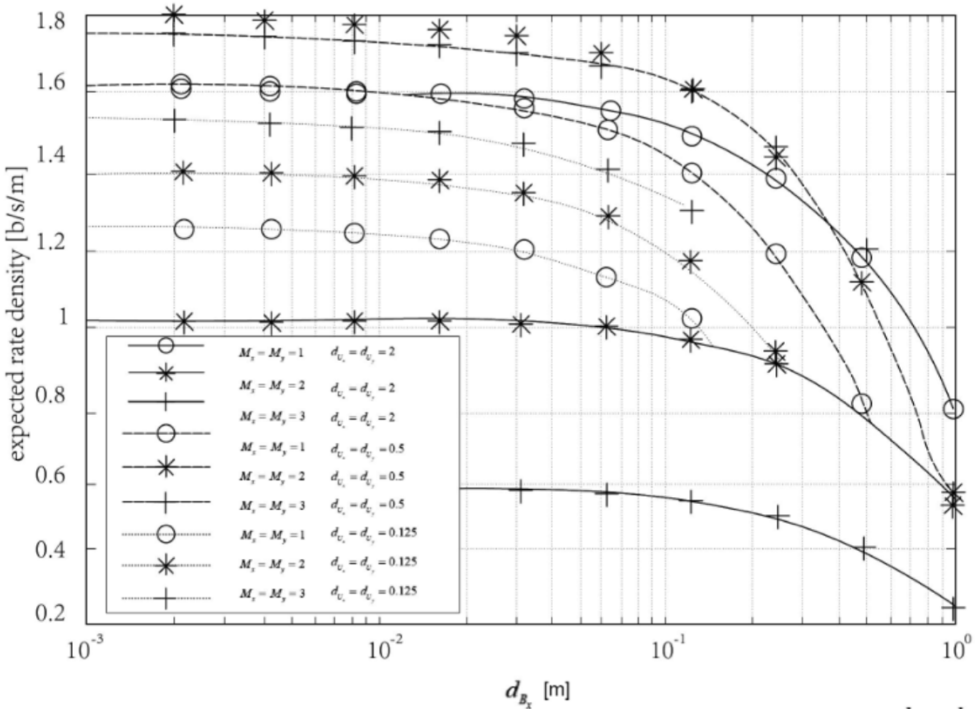

Figure 15 Expected rate density versus BS density for different values of UE density.

Figure 15 shows the expected rate density for $d_{U_x} = d_{U_y} = d_{B_x} = d_{B_y}$, different cluster sizes ($M_x = M_y = 1$ and $M_x = M_y = 4$, which, from (1), implies that $K_x = K_y = 1$ and $K_x = K_y = 4$, respectively), and different available power per meter. The most relevant conclusion of this figure is that, independently of the cluster size and the available power per meter, the expected rate density converges when the density increases, i.e., when $d_{U_x}, d_{U_y}, d_{B_x}, d_{B_y}$ decrease. Therefore, the rate of a particular UE decreases if both BS and UE density increase, as concluded in [8], [9]. However, there are strong differences between our model and the model in [8], [9]. One of these differences can be pointed out nothing that one of the conclusions of [8], [9] is that the system throughput increases linearly with densification for near-field path loss exponents greater than 2. In fact, this is the case depicted in Figure 15, which was obtained for $\gamma = 3$. However, with our model, the expected rate density converges with densification due to the use of fixed available power per meter and a minimum distance between BSs and UEs through the use of h=1.

Comparing now the different lines in Figure 16, we observe that, independently of the cluster size, the expected rate density increases with the available power. However, this increment has a limit, which is illustrated in Figure 16 with the curves for $\eta_x \to \infty$ and $\eta_y \to \infty$. In other

words, no matter how much power is available in the BSs, the expected rate density cannot be higher than that shown in the curves with $\eta_x \to \infty$ and $\eta_y \to \infty$. There curved were obtained assuming a null noise power, i.e., N=0, in which case the network is clearly interference limited.

The best cluster size depends on the available power. Specifically, for $\eta_x = \eta_y = 1$ and $\eta_x = \eta_y = 10$, the expected rate density is higher with $M_x = M_y = 1$ than with $M_x = M_y = 4$, although for $\eta_x = \eta_y = 100$ and $\eta_x \to \infty$ and $\eta_y \to \infty$ this order is reversed. This result highlights the need of increasing the cluster size with the available power in order to mitigate the effect of interference.

Comparing now the different lines in Figure 14, we observe that, independently of the cluster size, the expected rate density increases with the available power. However, this increment has a limit, which is illustrated in Figure 14 with the curves for $\eta_x \to \infty$ and $\eta_y \to \infty$. In other words, no matter how much power is available in the BSs, the expected rate density cannot be higher than that shown in the curves with $\eta_x \to \infty$ and $\eta_y \to \infty$. There curved were obtained assuming a null noise power, i.e., N=0, in which case the network is clearly interference limited.

The best cluster size depends on the available power. Specifically, for $\eta_x = \eta_y = 1$ and $\eta_x = \eta_y = 10$, the expected rate density is higher with $M_x = M_y = 1$ than with $M_x = M_y = 4$, although for $\eta_x = \eta_y = 100$ and $\eta_x \to \infty$ and $\eta_y \to \infty$ this order is reversed. This result highlights the need of increasing the cluster size with the available power in order to mitigate the effect of interference.

Probably, the most unforeseeable result shown in Figure 14 is that the expected rate density converges for $d_{B_x} \to 0$ and $d_{B_y} \to 0$ to the same value independently of the cluster size. The convergence point, however, increases with the available power. This points out that, in networks with very high density of BSs and UEs, it is beneficial to increase the available power, and the use of interference avoidance mechanism is not critical.

Due to this surprising result, one may wonder if the same behaviour is exhibited when only the BS density increases. This question in answered in Figure 17, when curves of the expected rate density with $\eta_x \to \infty$ and $\eta_y \to \infty$ are shown for fixed UE densities. In particular, the figure

shows results for all possible combinations of cluster sizes for $M_x = M_y = 1$ to $M_x = M_y = 3$ (let $M_x = M_y$ always be true) and inter-UE distances of $d_{U_x} = d_{U_y} = 0.125$, $d_{U_x} = d_{U_y} = 0.5$ and $d_{U_x} = d_{U_y} = 2$. In this case, all the curves converge when $d_{B_x} \to 0$ and $d_{B_y} \to 0$ but to different values. The optimum cluster size depends on the inter-UE distance.

4.2 Achievable rates in the limits of densification

a)

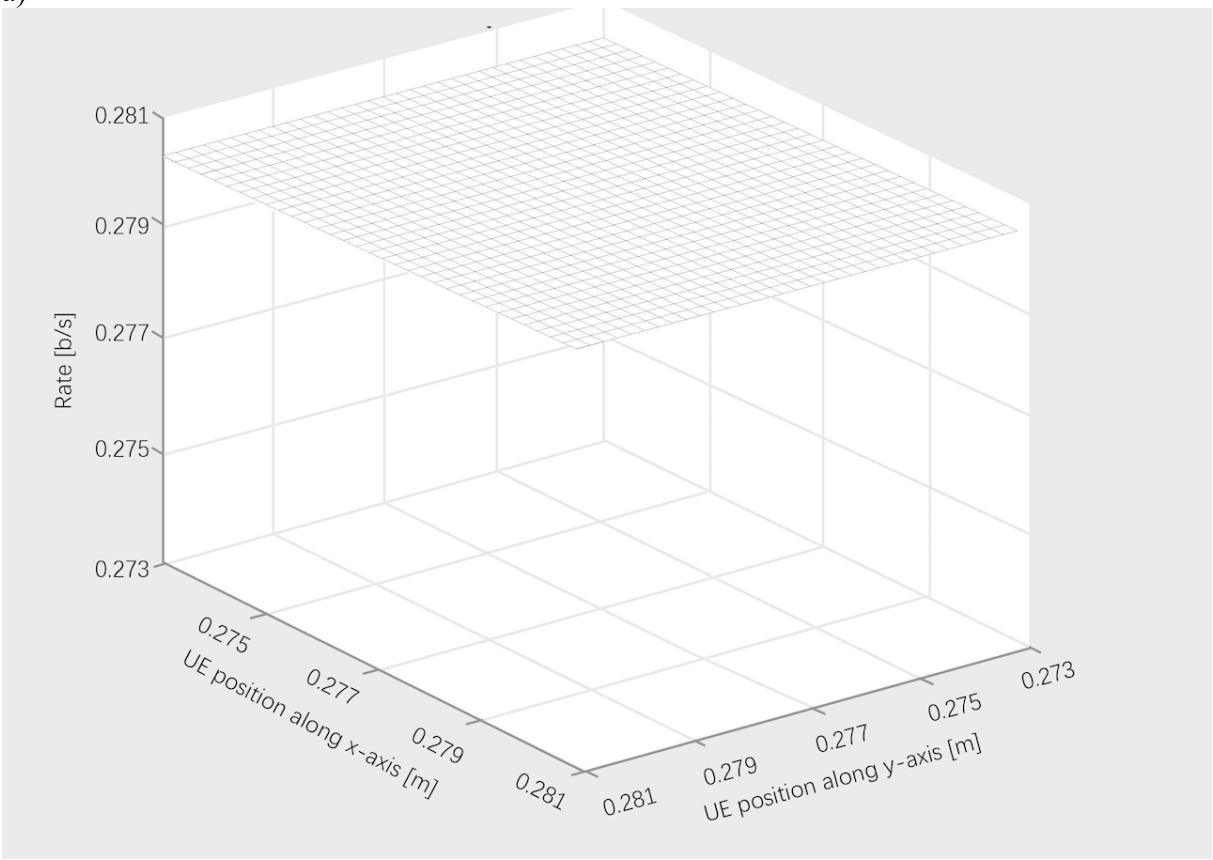

Figure 16 UEs achievable rate with respect to their location for dBx nearly equals to 0 and dBy nearly equals to 0 with overlapped cluster.

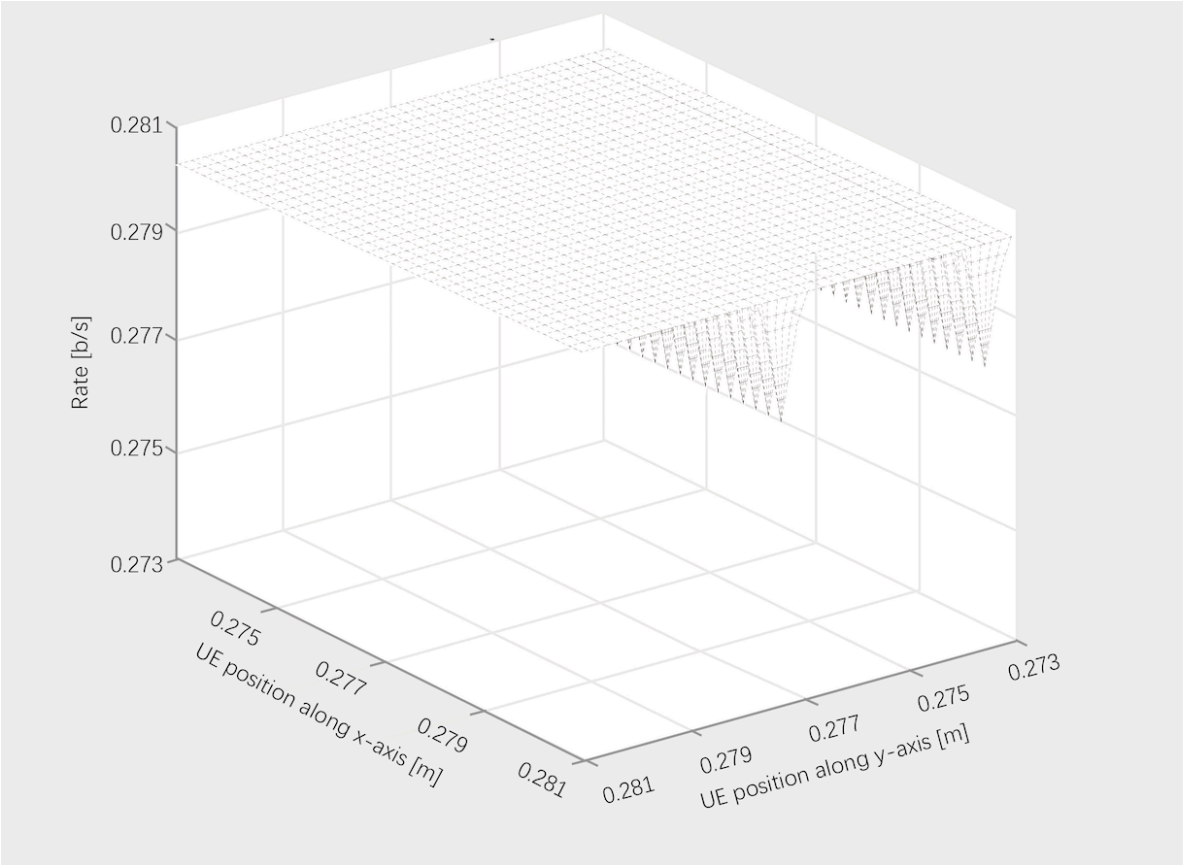

Figure 17 UEs achievable rate with respect to their location for dBx nearly equals to 0 and dBy nearly equals to 0 with non-overlapped cluster.

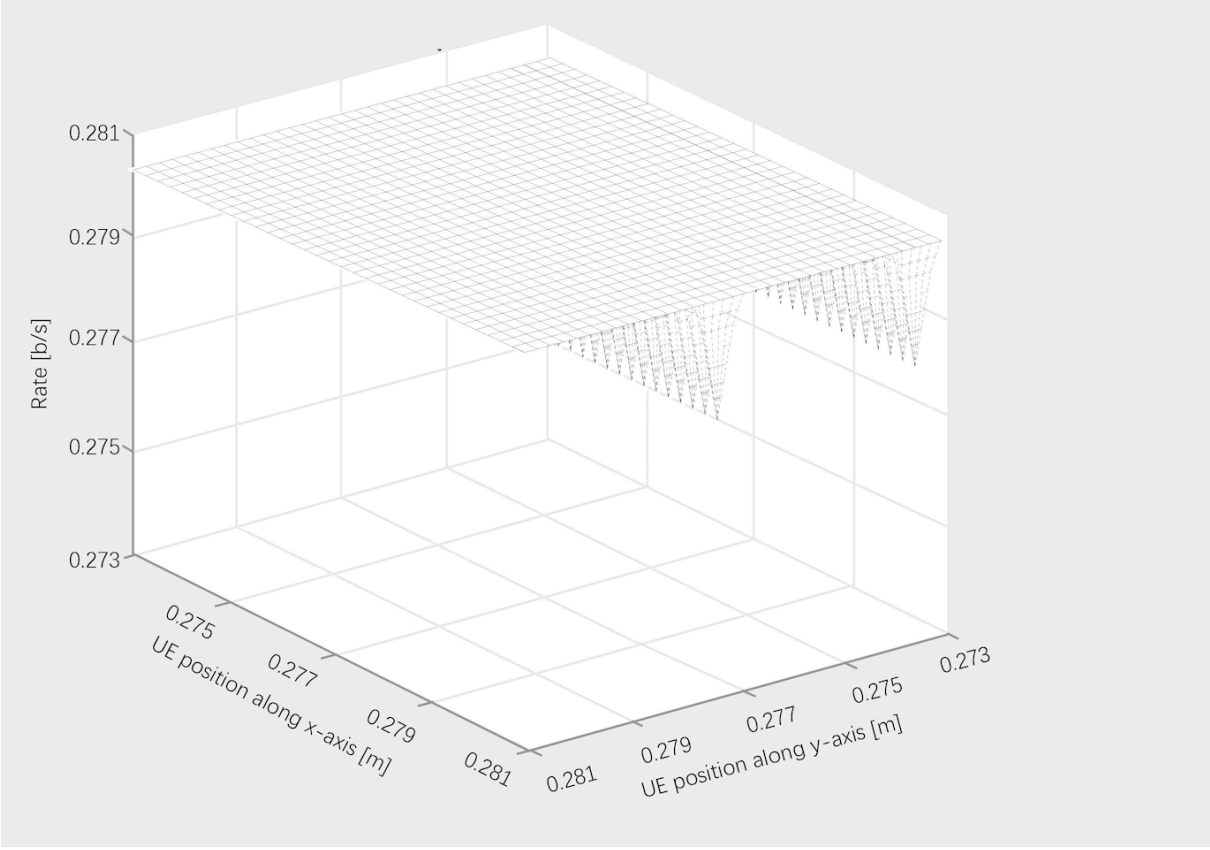

Figure 18 UEs achievable rate with respect to their location for dBx nearly equals to 0 and dBy nearly

equals to 0 with both overlapped and non-overlapped clusters.

In this section, we show results for the case $d_{B_x} \to 0$ and $d_{B_y} \to 0$. The rates were obtained using the achievable rates per resource element of the previous section, equally dividing the resource elements among the UEs that share serving BSs as deduced in the previous section, and assuming h=B=W=N=1 and $\gamma = 3$.

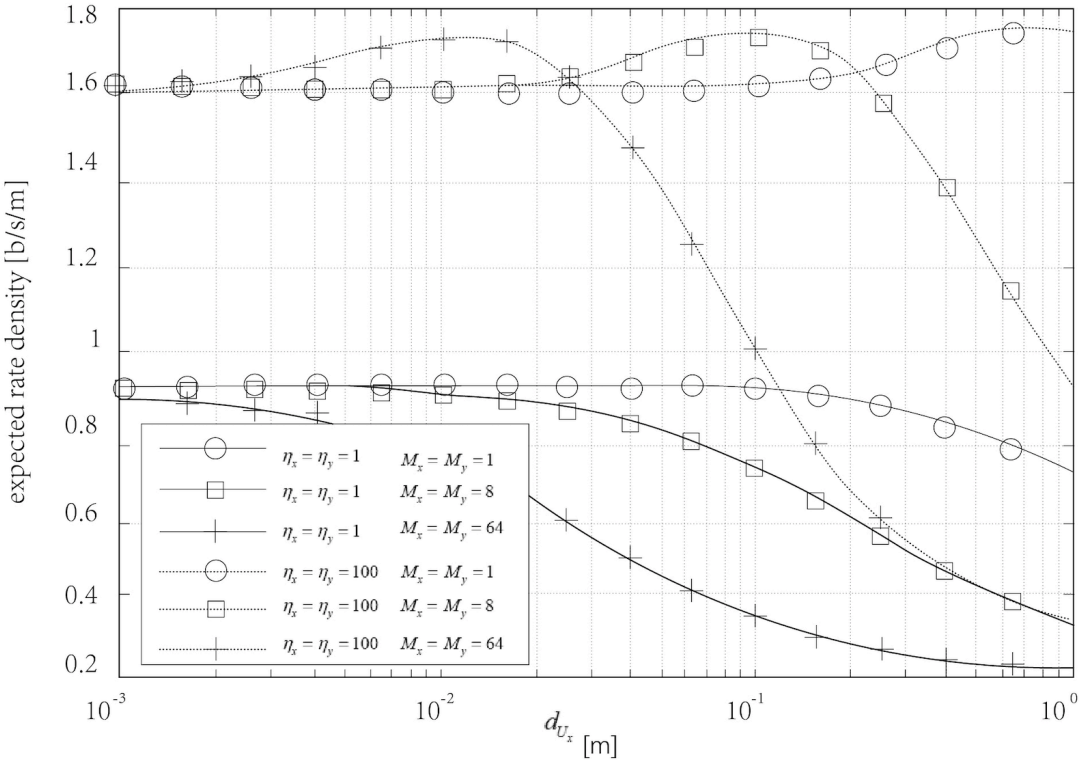

Figure 19 Comparison of energy components.

Fig 19 expected rate density with respect to d_{U_x} with overlapped clusters. (where $d_{U_x} = d_{U_y}$)

Figure 16,17,18 shows the achievable rates for different UE locations when $M_x = M_y = 4$, $d_{U_x} = d_{U_y} = 0.1$ and $\eta_x = \eta_y = 100$. This figure corresponds to the limit when $d_{B_x} \to 0$ and $d_{B_y} \to 0$ of Figure 2-13. As advanced in the previous section, the achievable rate with overlapped clusters converges to around 0.28b/s, independently of the UE position. Form the figure, it can be observed that the uniform rate achieved with overlapped clusters is the maximum rate achieved with non-overlapped cluster. Moreover, the performance of the non-overlapped clusters is damaged around the cluster borders, e. g., even when $d_{B_x} \to 0$ and $d_{B_y} \to 0$, although in the cluster centre the difference between the two types of clustering is

negligible.

he expected rate density at the limit of densification with overlapped clusters is presented in Figure 19, with respect to d_{U_x}, d_{U_y} and for different values of M_x M_y η_x and η_y. It is important to note that, since BS density is infinite, cooperation among BSs is essential for scenarios considered in this figure. In the $M_x = M_y = 1$ case, there is, however, no interference coordination. BSs cooperate for the transmission to only one UE, without considering any potential interference caused to other UEs. Conversely, in the $M_x = M_y > 1$ cases, in addition to cooperation to transmit to a UE, resources are divided among $M_x \times M_y$ UEs. Thanks to this, the sources of interference are distanced, although this is only beneficial if enough power is available in the UDE, as depicted by the different curves for $\eta_x = \eta_y = 1$ and $\eta_x = \eta_y = 100$ in Figure 19. This result has an interesting interpretation. Even if the density of BSs is infinity, a UDN with a finite available power along x-axis or along y-axis can be noise-limited.

Another important conclusion of Figure 19 is that, for a particular available power per meter along x-axis or along y-axis, the expected rate density converges to the same value when the UE density increases, independently of the amount of UEs. A similar result was obtained in the previous section, where we concluded that, for networks with very high density of BSs and UEs, it is beneficial to increase the available power, and the use of interference avoidance mechanism is not critical.

Chapter 5: Conclusion and Further Work

We have considered UDNs with densities approaching infinite that provide proportionally fair rates to the user equipment.

We find that though there are two types of clustering techniques, the performance of overlapped cluster is greater than or equal to the non-overlapped one, especially significant around the cluster borders and in denser networks, so in the future work, we would consider more about the overlapped clustering. What's more, when the distance between base station is nearly 0, the rates convergence to a certain value instead of infinite. And regardless of the cluster size and available power per meter, the expected rate density converges when density increases, and the convergence point increases with the available power. Because of this, in networks which are very high density of base stations and user equipment, it is beneficial to increase the available power.

In my model, I set the noise be a fixed constant, and in the future, I think we should make the noise part be more precise to make the model be more reliable.

References

[1] T. S. Rappaport, S. Sun, R. Mayzus, H. Zhao, Y. Azar, K. Wang, G. N. Wong, J. K. Schulz, M. Samimi, and F. Gutierrez, (2013) "Millimeter Wave Mobile Communications for 5G Cellular: It Will Work!" IEEE Access, vol. 1, pp. 335–349.

[2] S.N.M. Ruijsenaars, (2000)" On Barnes' Multiple Zeta and Gamma Functions",Advances in Mathematics.

[3] M. Agiwal, A. Roy, and N. Saxena, (2016) "Next Generation 5G Wireless Net- works: A Comprehensive Survey," IEEE Communications Surveys Tuto- rials, vol. 18, no. 3, pp. 1617–1655.

[4] GIMÉNEZ COLÁS, Sonia. Ultra Dense Networks Deployment for beyond 2020 Technologies. 2017. Tesis Doctoral.

[5] K. Kirsten and F. Williams, A Window into Zeta and Modular Physics. Cambridge, UK: Cambridge University Press, 2010.

[6] J. G. Andrews, F. Baccelli, and R. K. Ganti, (2011) "A Tractable Approach to Coverage and Rate in Cellular Networks," IEEE Transactions on Com- munications, vol. 59, no. 11, pp. 3122–3134.

[7] H.S.Dhillon, R.K.Ganti, F.Baccelli, and J.G.Andrews, (2012) "Modeling and analysis of K-tier downlink heterogeneous cellular networks," IEEE Iournal on Selected Areas in Communication, vol.30, no.3, pp.550-560.

[8] J.G.Andrews, X.Zhang, G.D.Durgin, and A.K.Gupta, (2016)"Are we approaching the fundamental limits of wireless network densification?," IEEE Communizations Magazine, vol 54, no. 10, pp. 184-190.

[9] X.Zhang and J. G. Andrews, (2015) "Downlink cellular network analysis with multi-slpe path loss models," IEEE transactions on Communications, vol. 63, no. 5, pp.1881-1894.

Acknowledgement

I would like to express my gratitude to all of the people who helped me to finish this project. First and foremost, I want to thank my supervisor. Since he was always patient and whenever I came across problems, he would help me to solve the problem. And in this process, I learnt a lot, not only the related knowledge, but the method to think to talk.

Appendix

You must include the following here, in the order of:

In this appendix, we will obtain a power allocation $x^*_{m_x,m_y}(s_x,s_y)$ that solves (27). To do that, we define

$$a_{k_x,k_y,m_x,m_y}(s_x,s_y) = L^{-1}_{(\lambda_{m_x}(s_x)+k_x),(\lambda_{m_y}(s_y)+k_y),m_x,m_y}(s_x,s_y)$$

$$b_{k_x,k_y,m_x,m_y}(s_x,s_y) = \sum_{i\in\mathbb{Z}\setminus\{0\}}\sum_{j\in\mathbb{Z}\setminus\{0\}} L^{-1}_{(\lambda_{m_x}(s_x)+iK_x+k_x),(\lambda_{m_y}(s_y)+jK_y+k_y),m_x,m_y}(s_x,s_y)$$

$$\sigma_{m_x,m_y}(x_{m_x,m_y},s_x,s_y) = \frac{\sum_{k_x=1}^{K_x}\sum_{k_y=1}^{K_y} a_{k_x,k_y,m_x,m_y}(s_x,s_y)x_{k_x,k_y,m_x,m_y}}{\frac{N}{P}+\sum_{k_x=1}^{K_x}\sum_{k_x=1}^{K_x} b_{k_x,k_y,m_x,m_y}(s_x,s_y)x_{k_x,k_y,m_x,m_y}}$$

and

and note that $x^*_{m_x,m_y}(s_x,s_y)$ also solves $\max_{x_{m_x,m_y}\in \mathrm{H}^{K_x,K_y}} \sigma_{m_x,m_y}(x_{m_x,m_y},s_x,s_y)$.

And then, we will show that there is a permutation function of $K_x \times K_y$ elements for each m_x, m_y, π_{m_x,m_y}, such that

$$a_{\pi_{m_x,m_y}(1),m_x,m_y}(s_x,s_y) \geq \ldots \geq a_{\pi_{m_x,m_y}(K_x\times K_y),m_x,m_y}(s_x,s_y)$$
$$b_{\pi_{m_x,m_y}(1),m_x,m_y}(s_x,s_y) \geq \ldots \geq b_{\pi_{m_x,m_y}(K_x\times K_y),m_x,m_y}(s_x,s_y)$$

where $\pi_{m_x,m_y}(1) = (k_x,k_y)$.

And if

$$a_{\pi_{m_x,m_y}(k),m_x,m_y}(s_x,s_y)(\frac{N}{P}+\sum_{j=1}^{k-1} b_{\pi_{m_x,m_y}(k),m_x,m_y}(s_x,s_y)) \geq b_{\pi_{m_x,m_y}(k),m_x,m_y}(s_x,s_y)\sum_{j=1}^{k-1} a_{\pi_{m_x,m_y}(j),m_x,m_y}(s_x,s_y),$$

then, we have that

$$\frac{\partial \sigma_{m_x,m_y}}{\partial x_{\pi_{m_x,m_y}(k),m_x,m_y}}(x_{m_x,m_y},s_x,s_y) \geq 0, \forall x_{m_x,m_y} \in \mathrm{H}^{K_x\times K_y}$$

Consequently, k^* is the largest $k \in \{1,\ldots,K_x \times K_y\}$ that satisfies the previous expression.